Deliverable Number:	D8.16
Deliverable Title:	Activation studies, radiation resistance

Delivery date:	Month 48
Leading beneficiary:	MTA EK (HAS, Centre for Energy Research)
Dissemination level:	Public
Status:	final
Authors:	Eszter Dian, HAS, Centre for Energy Research Esben Klinkby, DTU Dávid Hajdú, HAS, Centre for Energy Research Carsten Cooper-Jensen, ESS Katalin Gméling, HAS, Centre for Energy Research János Osán HAS, Centre for Energy Research Péter Zagyvai, HAS, Centre for Energy Research

Project number:	654000
Project acronym:	SINE2020
Project title:	Worldclass Science and Innovation with Neutrons in Europe 2020
Starting date:	1st of October 2015
Duration:	48 months
Call identifier:	H2020-INFRADEV-2014-2015

Funding scheme: Combination of CP & CSA – Integrating Activities

This project has received funding from the European Union's Horizon 2020 research and innovation programme under grant agreement No 654000

Abstract

The radiation shielding properties of concretes and other structural materials of shielding, e.g. metals are well-studied and commonly simulated, unlike to the dose consequences of their neutron activation. A detailed work was carried out on the neutron activation properties of three metal samples and three types of concretes, including the PE-B4C-concrete, developed in the European Spallation Source (ESS). The activity production in these samples was determined by neutron irradiation in the Budapest Research Reactor (BRR). PE-B4C-concrete showed significantly lower total activity concentration than its reference concrete. The impact of concrete composition in activation production was also demonstrated by activation simulations with the nominal composition - mostly limited to the bulk components - and multiple measured compositions of the concrete samples, using MCNPX and Cinder90. On this basis, realistic material cards were generated for activation simulations. The impact of concrete composition on decay gamma emission was also demonstrated in a maintenance case simulation of the ESS bunker. Decay gamma dose rates were found to be 29-72% higher with the use of the measurement-based input compositions, compared to the nominal ones, highlighting the importance of correct determination of trace elements in materials in relation to safety planning.

Acknowledgements

This project has received funding from the European Union's Horizon 2020 research and innovation programme under grant agreement No 654000. Computing resources were provided by DMSC Computing Centre (https://europeanspallationsource.se/data-management-software/computing-centre).

Table of Content

Introduction

The European Spallation Source (ESS) ERIC will be the brightest neutron source in the world [1]. Due to the high neutron fluxes with wide variety of spectra in the bunker, the different neutron guides and the instrument caves, an extensive and detailed safety planning is essential for all the components of the facility exposed to radiation. Moreover, special attention should be paid on the newly developed and applied solutions and materials of radiation protection. One of them is the so-called PE-B4C-concrete [2]. This concrete has been developed in ESS from an ordinary concrete, - in the followings referred to as 'Reference concrete', - by replacing part of the pebble-content with B_4C grains and polyethylene (PE) beads, giving in total ~10 w% of the new mixture (0.76% and 10.2%, respectively) [3]. The shielding properties of the PE-B4C-concrete [3] and other concretes are well-investigated [4][5] and simulated with different Monte Carlo codes [6]. However, the effects of activation products on nuclear safety is known, but much less studied [7][8][9]. Most of the concrete compositions (in MCNP terms: 'material cards'), that are currently available for simulation purposes, are limited to the bulk components of the concrete (i.e. the nominal composition given by the manufacturer), that determine their shielding properties, but exclude the trace elements that may be dominant as a result of neutron activation [10]. The published studies in shielding material activation mostly focus on long-lived radioisotopes and radioactive waste management considerations, highlighting the role of cobalt and europium content of the concretes [11][12]. However, the neutron activated materials may have short-term effects as well in terms of occupational exposure. For example, maintenance of neutron scattering instruments and beamlines usually performed with a few days of cooling after closing the beam, when the dose consequences of decay gamma radiation of the short-lived activation products from shielding and other instrument components should be considered.

The two-fold aim of the current study is to determine the neutron activation properties of the newly developed PE-B4C-concrete in comparison with other common shielding concretes, and to facilitate more realistic Monte Carlo neutron activation simulations of concretes and other structural components of neutron shielding (e.g. metals). For this purpose, three metal samples: aluminium, copper and stainless steel; and three concrete samples were studied: the above introduced PE-B4C-concrete and its Reference concrete, and a general concrete produced by Skanska company, - referred to as 'Skanska concrete' in the followings, - that is currently used in ESS. For this purpose, neutron irradiation experiments were performed in the vertical irradiation channels of the Budapest Research Reactor (BRR) [13] with different neutron spectra, determining the activation properties of all the listed concretes and metals.

Fulfilling the second aim of this study, the initial compositions of concrete samples were also measured with different analytical techniques, in order to provide detailed data for realistic activation calculations: Prompt-Gamma Activation Analysis (PGAA) [14] was used along with Neutron Activation Analysis (NAA) [15] in the BRR. PGAA is suitable to measure the bulk components of concretes which has lower atomic number, while trace elements can be effectively measured with NAA. However, the high cost and off-site character do not make it possible to apply neutron activation techniques for continuous quality assurance measurements during construction. To examine a possible solution, the widely used energy-dispersive X-Ray Fluorescence (EDXRF) [16] measurements were also performed, and were compared to the results of neutron activation analysis [17][18].

Similar activity and composition measurements were also carried out on metal samples, except for the PGAA, because no additional information was expected from that method. As the amount of metals as structural materials is significantly smaller than concretes, and the trace elements of metals are more studied, simulations of metals were excluded from this work, but they could be performed based on the presented results in the future.

In order to study the impact of the initial concrete composition on activation simulations, the performed neutron irradiation measurements were reproduced using MNCPX [19] jointly with Cinder90 [20], using the different measured and nominal concrete compositions as inputs. On the basis of the obtained results, recommended material cards were developed for activation simulations for all the studied concretes, best fitting and so being validated by the measured activities.

Finally, in order to demonstrate the impact of concrete activation not only in terms of activity and waste production, but the dose consequences as well, a simulation study was performed in the bunker of the ESS. A realistic irradiation scenario was simulated with the application of the generally used nominal and a measurement-based composition of the Reference concrete in a single bunker wall. The decay gamma dose rates, caused by the activated wall were determined for the whole bunker hall after three days of cooling, representing a maintenance case.

With this study, the importance of trace elements in safety calculations is highlighted, and a generally applicable method is presented for the development of simplified but realistic input compositions for neutron activation simulation purposes.

Activity and composition measurements

The compositions of the metal- and concrete samples were measured with three analytical techniques: Neutron Activation Analysis (NAA) [15], Prompt-Gamma Activation Analysis (PGAA) [14] and energy-dispersive X-Ray Fluorescence (EDXRF) [16], and their activation properties were determined as well from neutron irradiation experiments in the BRR.

Analytical techniques and irradiation experiments

Neutron irradiation and NAA measurements

NAA measurements had a two-fold aim: to determine the activation properties of the studied shielding and structural materials, and also to provide realistic input data on the composition of these materials for Monte Carlo activation simulations.

Three concrete and three metal samples were provided by the ESS. The metal samples were 5 × 5 × 5 mm^3 cubes, 4 replicates from each material, while the concrete samples were given as grist. For the NAA measurements the samples were prepared this way: ~0.1 g sample material was measured of each concrete to high-purity quartz ampoules using a Mettler-Toledo XPE 26 microbalance (<0.7 µg reproducibility).

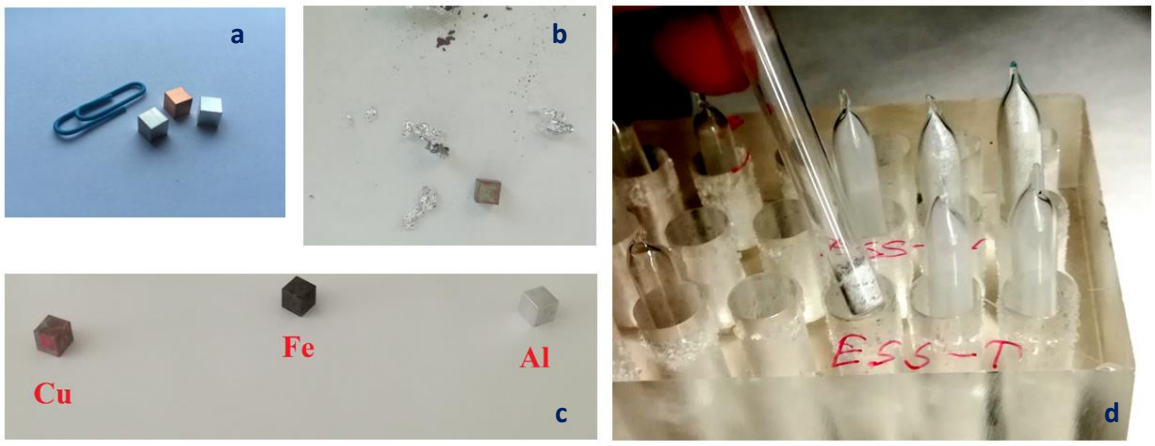

Figure 1 Initial (a) and irradiated metal samples (b, c), and encapsulated concrete samples prepared for irradiation (d).

Two set of samples were prepared and placed to 10 cm long aluminium tubes (see Figure 2) and irradiated in the water-filled, vertical irradiation channels of the Budapest Research Reactor (BRR) [13]. The first set was irradiated in a rotated, well-thermalized irradiation channel (referred to later on as 'Thermalized channel') located in the beryllium reflector around the reactor core (see Figure 3). The second set was placed into a channel in the reactor core, having higher fast/thermal

neutron flux ratio (referred to as 'Fast channel'). The irradiation time was 2 hours in all sets of samples, except for the metal samples in the Fast channel, which took only 10 minutes, due to large mass and so high total activity of the samples. This is the technically minimum duration of irradiation in the vertical channels. The parameters of the neutron flux were monitored with Bare Triple-Monitor method [21] and are presented in Table 1.

Figure 2 Aluminium sample holder.

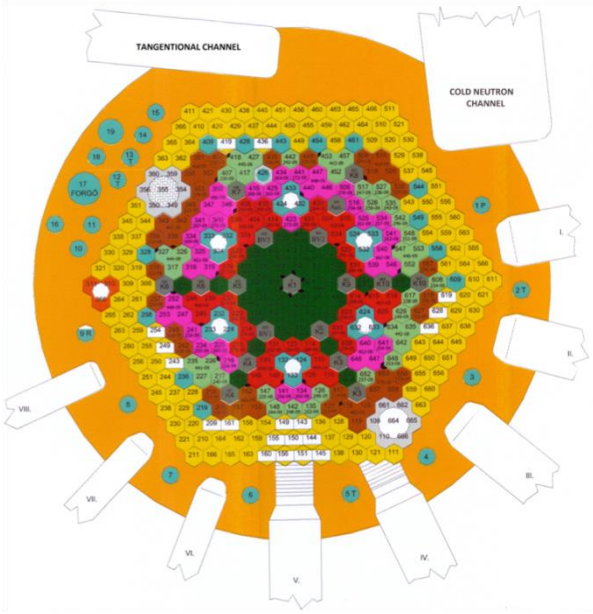

Figure 3 Zone map of BRR [13].

Table 1 Measured neutron fluxes in the vertical irradiation channels of BRR [13]. (Uncertainties are 15-20%.)

	Thermalized channel	Fast channel
Thermal flux [cm^{-2} s^{-1}]	2.00E+13	5.00E+13
Epithermal flux [cm^{-2} s^{-1}]	4.30E+11	3.80E+12
Fast flux [cm^{-2} s^{-1}]	1.30E+12	4.70E+13

The activity of the irradiated samples were determined by measuring their gamma response with a Canberra HPGe gamma-detector (p-type detector, 36% relative efficiency, 1.75 keV/1332.5 keV resolution; connected to Ortec 502 MCA-2) in a low background measurement chamber. The first measurements were performed after 1-4 days of cooling, as otherwise the dead time would have been too high, due to the high initial activity of the samples. Samples were measured 2-5 times in a ca. 3-week long time interval, to determine their decay characteristics. Measurement time increased from

10 minutes to 2 hours in this period. The optimal detector-sample distances and measurement time were chosen for each measurement. The copper samples required longer cooling time and so were measured only twice in the end of the studied time period. The details of activity measurements are given in Appendix B and D, Table B 1 - Table B 5 and Table A 1 - Table A 6 for concrete and metal samples, respectively. The elemental compositions of the samples were also determined with Hypermet PC [15] and KayZero for Windows 3.06 program [22].

PGAA composition measurements

PGAA elemental analysis was also performed on the concrete samples in the PGAA station of the BRR [14].For this purpose, 6 g-portions of concretes were weighed and heat-sealed into Teflon bags. The sample is irradiated in a guided neutron beam, where the neutron flux at the sample position was about 9.6×10^{7} $cm^{2}s^{-1}$. The cross-section of the neutron beam was adjusted to 20×20 mm^{2} to optimize the prompt gamma count rate. During the neutron irradiation, the prompt gamma radiation, emitted from the neutron capture, was detected with a High-Purity Germanium (HPGe) detector, surrounded by a Bismuth Germanate (BGO) scintillator and 10 cm thick lead shielding. Each samples were irradiated for 10 hours. The signals were processed with a Canberra AIM 556A multichannel analyser. The spectra were evaluated with Hypermet-PC gamma spectroscopy software. The element identification was performed with the ProSpeRo program, utilizing the following prompt-gamma analysis library: [23]. The measured compositions of the concrete samples are presented in Table C 1 - Table C 3.

EDXRF composition measurements

As a relatively fast and low-cost technique, energy-dispersive X-ray fluorescence (EDXRF) [16] spectroscopy analysis was also carried out on the concrete and metal samples in the Nuclear Science and Instrumentation Laboratory of the IAEA [24].

The metal samples, $5 \times 5 \times 5$ cm^{3} cubes of aluminium, copper and steel were measured with a handheld XRF device (Niton X3Lt GOLDD+, Thermo Scientific). The measured compositions of the metal samples are presented in Table C 1 - Table C 3.

.

Figure 4 Ground concrete samples and pellets for EDXRF measurement. (a) raw grain (b) fine grain, (c) pellet of Reference concrete and (d) pellet of PE-B4C-concrete.

In case of the concrete samples, before the measurement, they were ground with a ball grinder using tungsten carbide (WC) balls and mortars to increase the homogeneity of the grist samples. The material used for grinding was considered during evaluation of elemental concentrations. After addition of 0.25 g wax, the samples were pressed to 2.5 g pellets. Three samples were prepared from all of the concretes and then measured with a triaxial polarizing EDXRF device (Epsilon5, PANalytical, The Netherlands) [25]. The instrument is equipped with a 100-kV X-ray tube, a series of secondary targets and an HPGe detector with high efficiency for hard X-rays. Each sample was measured under ten different conditions using secondary targets suitable for different groups of elements. Concentrations were calculated using the built-in software based on all ten spectra for each sample. The calibration curves used for the concrete samples were generated from measurements of several geological certified reference materials. Using several secondary targets is advantageous since it allows a full elemental analysis of the samples for elements from Na to U, considering major elements as present in the common oxide forms [26]. The condition using a 100-keV excitation and a Barkla polarizing secondary target makes it possible to quantify lanthanide elements based on their K lines. EDXRF in general has a high dynamic range covering major to trace elements. The measured compositions of the concrete samples are presented in Table C 1 – Table C 3.

Determination of activities

Activities in metal samples

The gamma spectra of the metal samples were recorded 2-5 times during a 3-week follow-up period after their irradiation. Gamma spectroscopy analysis was performed from each set of recorded data, determining the activities in isotopic level. The measured activities are presented in Table A 1-Table A 6. As the focus of the current task was more on the concrete activations, the results of metal irradiations are only briefly discussed. However, these measurements served as excellent preparations for the concrete measurements, giving valuable experience for developing the measurement and analysis methods later applied for the concretes.

The radiation production in the metal samples was studied in terms of short-term and long-term activity, i.e. maintenance and measurement scenarios and radioactive waste production as well. A few of the measured results are presented below.

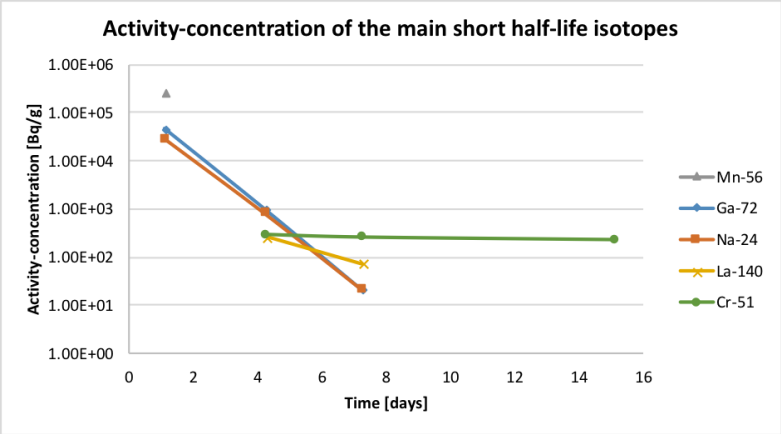

Figure 5 Short-lived radioisotopes in aluminium, irradiated in the Thermalized channel.

In Figure 5 it is shown that in accordance with the expectations, the short-term activity concentration in the aluminium is dominated by Mn-56, and trace elements like Ga-72, and Na-24. Cr-51 and Fe-59 become the dominant source of activity concentration after 5 days of cooling.

In the case of copper, activity concentration is dominated by the Cu-64. Only Ag-110m has any comparable activity concentration, while all the other detected isotopes have one order-of-magnitude smaller activity concentration.

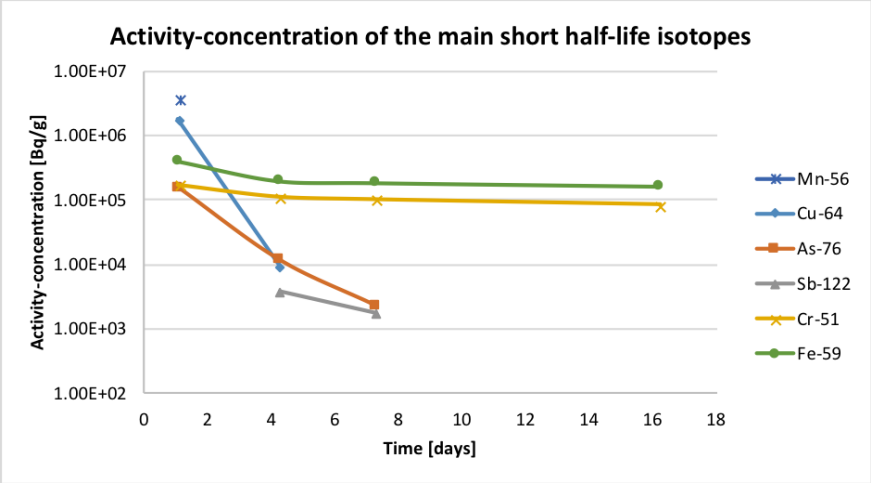

Figure 6 Short-lived radioisotopes in stainless steel, irradiated in the Thermalized channel.

In Figure 6 it is shown that the major contributors to the activity in stainless steel at the beginning of cooling time were Mn-56 and Cu-64, although the uncertainties of the measurement were high for the latter. The isotopes with longer half-life, such as Cr-51 and Fe-59 became dominant contributors of the activity concentration after 3 days of cooling. The surely present Ga-72, which has longer half-life, is shadowed by the overlapping intense gamma line of the Mn-54.

The long-lived isotopes of these samples are summarised in Figure 7, their activities are extrapolated to one year of cooling from the end of irradiation. It is shown that for the same volume of samples stainless steel has the highest long term activation. It is also shown that in accordance with the expectations, for all metals Co-60, and for stainless steel Mn-54 as well are the dominant sources of activity

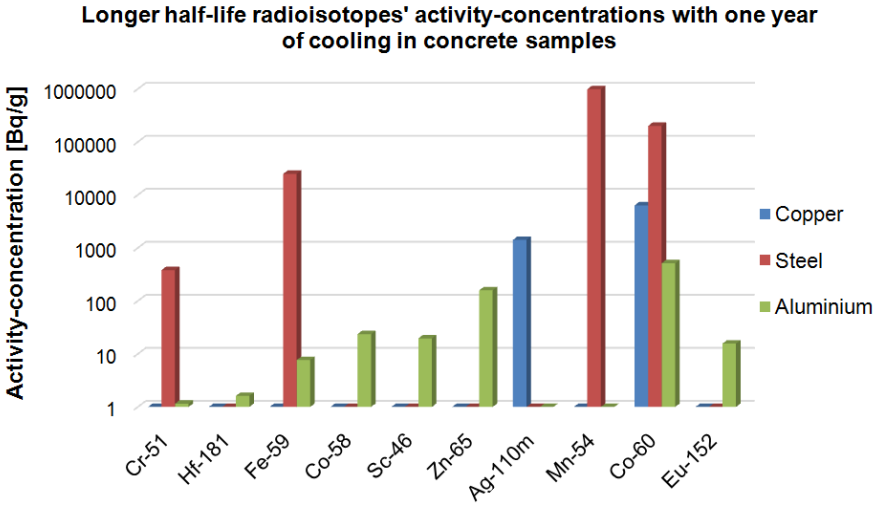

Figure 7 Activity concentrations of the dominant medium- and long-live isotopes in the three metal samples, extrapolated to one year of cooling after the irradiation.

Activities in concrete samples

The activities of the concrete samples were recorded 5 times during a 2 week follow-up period after their irradiation. As an example, the measured activities of the PE-B4C-concrete, irradiated in the Fast channel is presented in Table 2. The rest of the results are shown in Table B 1-Table B 5.

Table 2 PE-B4C sample irradiated in Fast channel.

Measurement		1		2		3		4		5	
Isotope	$T_{1/2}$ [days]	Act. conc. [Bq/g]	*Unc [%]*	Act. conc. [Bq/g]	*Unc. [%]*	Act. conc. [Bq/g]	*Unc. [%]*	Act. conc. [Bq/g]	*Unc. [%]*	Act. conc. [Bq/g]	*Unc. [%]*
K-42	**0.5**	5.27E+05	*12*	2.11E+05	*12*	-	-	-	-	-	-
Na-24[7]	**0.6**	1.02E+07	*1*	4.66E+06	*1*	1.02E+04	*2*	-	-	-	-
W-187	**1.0**	1.06E+06	*2*	7.30E+05	*2*	1.62E+04	*3*	-	-	-	-
As-76	**1.1**	8.82E+04	*13*	3.97E+04	*19*	-	-	-	-	-	-
La-140	**1.7**	2.14E+05	*3*	1.92E+05	*3*	1.59E+04	*1*	2.76E+03	*2*	1.22E+03	*3*
Sm-153	**1.9**	3.47E+05	*4*	2.90E+05	*4*	4.17E+04	*3*	9.05E+03	*4*	3.67E+03	*5*
Np-239[1]	**2.4**	-	-	-	-	7.58E+03	*4*	1.80E+03	*13*	1.01E+03	*15*
Sb-122	**2.7**	3.52E+04	*16*	3.61E+04	*16*	6.77E+03	*6*	2.78E+03	*6*	1.45E+03	*9*
Sc-47[2]	**3.3**	-	-	1.74E+04	*17*	9.07E+03	*5*	6.01E+03	*3*	3.92E+03	*3*
Yb-175	**4.2**	-	-	-	-	1.70E+04	*13*	9.37E+03	*12*	5.85E+03	*16*
Ca-47	**4.5**	-	-	-	-	3.54E+03	*6*	2.39E+03	*8*	1.46E+03	*4*
Lu-177	**6.7**	-	-	-	-	7.25E+03	*21*	0.00E+00	*10*	4.15E+03	*12*
Ba-131	**12**	-	-	-	-	7.67E+03	*2*	7.16E+03	*1*	5.65E+03	*1*
Rb-86	**19**	-	-			3.40E+04	*7*	4.16E+04	*3*	3.62E+04	*5*
Pa-233[3]	**27**	-	-	2.78E+04	*23*	1.38E+04	*3*	1.59E+04	*3*	1.37E+04	*3*
Cr-51	**28**	-	-	-	-	4.81E+04	*4*	5.43E+04	*3*	4.73E+04	*2*
Yb-169	**32**	-	-	-	-	1.87E+03	*18*	1.76E+03	*11*	1.62E+03	*10*
Ce-141	**33**	-	-	-	-	5.26E+03	*7*	5.08E+03	*3*	4.40E+03	*3*
Hf-181	**42**	-	-	-	-	3.26E+03	*8*	4.02E+03	*2*	3.53E+03	*2*
Fe-59	**45**	-	-	6.14E+04	*13*	2.89E+04	*1*	3.67E+04	*1*	3.29E+04	*1*
Sb-124	**60**	-	-	-	-	1.44E+03	*9*	1.95E+03	*3*	1.74E+03	*3*
Zr-95	**64**	-	-	-	-	-	-	7.78E+02	*13*	7.10E+02	*12*
Sr-85	**65**	-	-	-	-	9.60E+02	*15*	9.60E+02	*10*	8.82E+02	*9*
Co-58[6]	**71**	-	-	-	-	-	-	6.46E+02	*16*	5.77E+02	*21*
Tb-160	**72**	-	-	-	-	-	-	2.77E+03	*5*	1.74E+03	*7*
Sc-46[4]	**84**	-	-	5.73E+04	*13*	3.32E+04	*1*	4.21E+04	*1*	3.87E+04	*1*
Ta-182	**114**	-	-	-	-	3.21E+03	*25*	3.47E+03	*3*	3.34E+03	*4*
Zn-65	**244**	-	-	-	-	3.67E+03	*13*	4.84E+03	*6*	4.40E+03	*7*
Mn-54[5]	**312**	-	-	-	-	6.79E+03	*7*	8.47E+03	*3*	7.99E+03	*3*
Cs-134	**754**	-	-	-	-	2.42E+03	*6*	2.84E+03	*3*	2.47E+03	*3*
Co-60[8]	**1924**	-	-	-	-	2.92E+03	*3*	3.88E+03	*2*	3.59E+03	*2*
Eu-152	**4941**	-	-	-	-	3.46E+03	*7*	4.31E+03	*5*	4.36E+03	*2*
Total*		**1.25E+07**		**6.32E+06**		**3.36E+05**		**2.78E+05**		**2.39E+05**	

*Sum of the activity concentrations of the listed radioisotopes

On the basis of the HPGe activity measurements in total, 32 gamma-emitting radioisotopes were identified, most of the produced via (n,γ) reaction, with a few marked exceptions. These reactions occur in the other measured datasets as well.

[1]Np-239: Descendant of ^{239}U, generated by thermal neutron activation from natural uranium content (^{238}U, 99.3 % of natural U).

[2]Sc-47: Product of fast neutron activation of ^{47}Ti (natural abundance in Ti: 7.3%) Accordingly, the activity of Sc-47 was higher in the samples activated in the Fast channel.

[3]Pa-233: Descendant of ^{233}Th, generated by thermal neutron activation of natural thorium content (^{232}Th, 100 % of natural Th).

[4]Sc-46: This radionuclide can be generated in two different processes: from ^{45}Sc (100% of natural Sc) by thermal neutron activation and from ^{46}Ti (8% of natural Ti) by fast neutron activation.

[5]Mn-54: This is the fast neutron activation product of ^{54}Fe (natural abundance in Fe: 5.8%) Accordingly, the activity of Mn-54 was higher in the samples activated in the Fast channel.

[6]Co-58: Product of fast neutron activation of ^{59}Co (natural abundance in Ti: 100%) and from ^{58}Ni (natural abundance in Ni: 68%). Accordingly, it was detectable only in the samples activated in the Fast channel.

[7]Na-24: Apart from its generation from stable Na-23 (100%), this radionuclide also can also be produced from Al-27 via (n,α), a relatively low threshold reaction.

[8]Co-60: This radionuclide also can also be produced from Cu-63 via (n,α), a relatively low threshold reaction.

It was found for all the samples, that, Na-24 and W-187 were the dominant sources of activity in the first few days of cooling, while Co-60 and Eu-152 are giving the majority of the total activity in long-term, in accordance with the expectations.

Determination of key radioisotopes

On the basis of the HPGe activity measurements 32 gamma-emitting radioisotopes were identified. As ESS is planned to be decommissioned after 5 years cooling time once its operation has ended [1], activity-concentrations of these isotopes were extrapolated with the decay equation to 1- and 5 years of cooling from the last two measurement points - when the measurements of long-lived isotopes were not affected significantly by the short-lived ones. Neutron activations simulations are most commonly performed with the joint use of MCNPX simulations and Cinder90 calculations. However, Cinder90 tends give an overflowed, hardly searchable inventory. On the basis of the measured activities it was found, that out of the 32 identified gamma emitting radioisotopes 15 isotopes composed the majority – at least 83% - of the total activity in all of the data points (both for measured and calculated ones. For the fast, simple and reliable comparison the simulated data, these 15 isotopes were identified as 'key isotopes', and so in the followings 'total activity' will be used as the sum of the activity of these isotopes.). The key isotopes and their decay in an irradiated PE-B4C-concrete sample are presented in Figure 8.

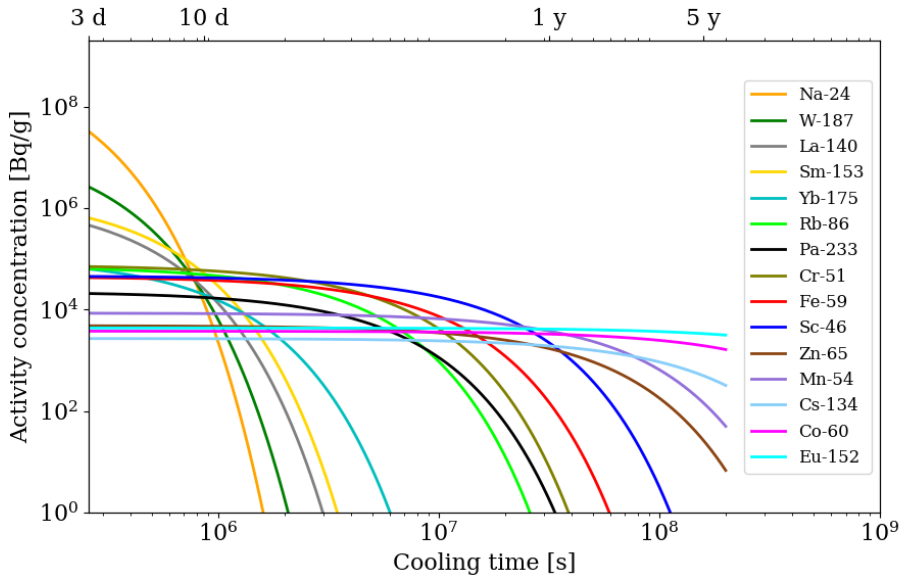

Figure 8 Decay curves of the 15 key radioisotopes of PE-B4C-concrete after irradiation in the Fast channel, extrapolated from measured data.

The 14 elements from which these key radioisotopes activated from - as iron is the parent element of both Fe-59 and Mn-54 - were also identified, and kept in the focus of composition measurements of concrete samples.

Decay of activated concrete samples

The decay the activated concrete samples was followed for a 2-3 weeks long cooling period. The measured activities of the three samples irradiated in the Thermalized and Fast channels are presented in Figure 9 and Figure 10, respectively.

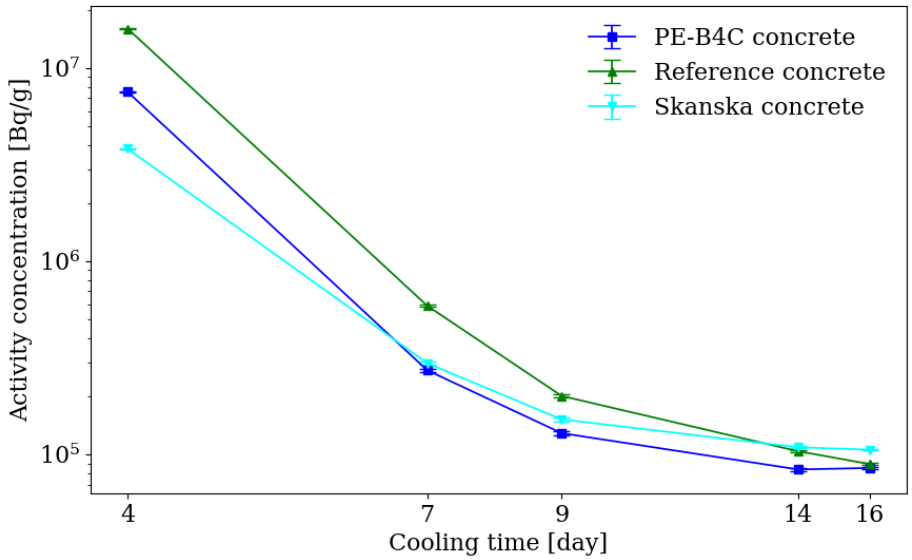

Figure 9 Measured decay profile of the 3 different concretes after irradiation in the Thermalized channel. The statistical uncertainties are too small to be discernible. The measured points are connected for better visibility.

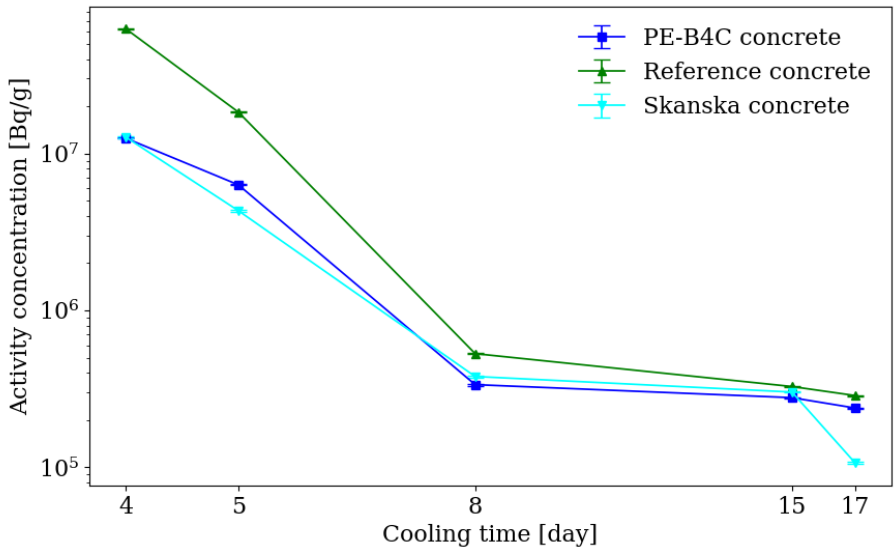

Figure 10 Measured decay profile of the 3 different concretes after irradiation in the Fast channel. The statistical uncertainties are too small to be discernible. The measured points are connected for better visibility.

It was shown, that in accordance with the expectations, the measured total activity of the newly developed PE-B4C-concrete is consequently lower than that of the Reference concrete for the whole studied time period in both sets of measurements and significantly lower during the first week after irradiation. PE-B4C-concrete produced ~53-54% and 66-80% lower activity during the first week of cooling for the Thermalized and Fast channels, respectively. For this reason, PE-B4C-concrete is proven to be more advantageous in terms of neutron induced decay gamma emission, especially for a few days of cooling, i.e. in case of maintenance. However, comparing the decay profiles of the PE-B4C- and the Reference concrete with that of the Skanska concrete, it is also revealed that the decrease in neutron-induced activity in the Skanska concrete, compared to the Reference concrete, is in the same range that in the PE-B4C-concrete: ~50-76% and 76-80% during the first week of cooling for the Thermalized and Fast channels, respectively. This indicates that the remnant activity of a concrete can be significantly reduced with the application of polyethylene and boron-carbide, although, the variation of activity production due to the different initial concrete types can already be within the same range, highlighting the importance of the initial composition.

Measured compositions and their impact on the activation simulation

Metal compositions

The compositions of the metal samples were determined with NAA and EDXRF analysis. The compositions are presented in Table A 8 - Table A 10. As the focus of the current task was more on the concrete activations, the measured compositions are not further used in any simulations. However, it was shown that both methods provide extensive data of trace elements, compared to the nominal composition, involving the parent elements of the long-term dominant Co-60.

Concrete compositions and material cards

The composition of the concrete samples was determined via PGAA, NAA and EDXRF analytical measurements, providing detailed input data for Monte Carlo neutron activation simulations. The compositions measured with each method are presented in Table C 1 - Table C 3. It is revealed, that the combination of PGAA and NAA measurements provided detailed and reliable data on the composition: PGAA giving the content of the bulk elements and the NAA giving the trace elements. However, the NAA method may be less accurate for elements with isotopes produced via multiple reaction channels. Also in PE-B4C-concrete H, C and B form a special group of bulk elements, as they are the elements of the additional components. In the nominal composition their theoretical value is indicated, which are 1.5-3 times underestimated by the PGAA measurements. In case of boron, it can occur due to the high boron content, which exceeds the limits of the technique. Other problem can

be the representative sampling, as only a low amount of sample was measured and plastic components do not form a homogenous mix with the concrete.

EDXRF measurements were also performed, providing input data both on bulk and trace elements above Na. Energy-dispersive X-ray fluorescence spectroscopy measurements show good agreement with the results of activation analysis for most of the elements. However, the parent elements of few key isotopes were not measurable: Sm and Yb were under detection limit of EDXRF, 2 and 20 ppm, respectively. Furthermore, the two most important elements generating long-lived isotopes were also not detected: Eu concentration found to be under the detection limit of 1 ppm and Co was not measurable due to severe spectral overlapping with the high iron concentration of the samples. For this reason, although EDXRF is an easy, relatively cheap technique for the quality assurance of concretes, it may not be adequate for shielding which will be posed to high neutron flux. The use of wavelength-dispersive XRF (WDXRF) might overcome the difficulty with Co due to its high spectral resolution.

Material cards for activity simulations

On the basis of the measured compositions and the activity simulations performed with the above described measured compositions, combined input compositions were constructed for the PE-B4C- and the Reference concrete, that sufficiently reproduce the measured activities, and therefore recommended for further activation simulations (referred to as 'recommended composition' in the followings) for e.g. radiation safety planning. The compositions were constructed with the following baselines:

1) The initial compositions consist of the nominal composition and the parent elements of the key isotopes.

2) For each element a measured value was preferred if it was available. As (in this unique case) the EDXRF analyses were performed with the most number of samples, the EDXRF produced values were favoured as default against other measured results, considering the better statistics.

3) NAA produced values were considered for elements in very low amount (10^{-4} w%), as in this particular case NAA provided lower detection limit than EDXRF, giving presumably more precise values.

4) When the different methods provided conflicting results - mostly due to the general inhomogeneity of the samples -, the more conservative values were selected.

5) Finally, as the oxygen content highly changes in the concrete, and has no activation product with any considerable gamma decay, any discrepancies due to the limited number of elements in the composition were added to the oxygen content, to complete the composition to 100% in mass.

The created recommended compositions were validated via the MCNPX simulations of the performed neutron irradiation experiments. No specific recommended composition was developed for the Skanska concrete, due to the lack of nominal composition. However, the PGAA and NAA based measured composition was proven to be adequate for activity simulations (See next section). The recommended composition of all concretes are presented in Table 3 in ready-to-use MCNP material card style, thus '-' indicates weight fraction. These are simplified, realistic compositions, recommended for activity simulations.

Table 3: Measurement-based compositions in MCNP material card style, recommended for neutron activation simulations. '-' indicates 'weight fraction'.

Element	Element ID	Weight fraction		
		PE-B4C-concrete	Reference concrete	Skanska concrete
H	1001	-1.2633E-02	-6.0087E-03	-3.46E-03
B	5000	-2.0000E-03	-2.4900E-05	-2.52E-05
C	6000	-5.4583E-02	-	-5.46E-03
O	8016	-4.6618E-01	-4.8801E-01	-4.96E-01
Na	11000	-1.2910E-02	-1.9676E-02	-5.57E-03
Mg	12000	-9.8257E-04	-9.5302E-03	-
Al	13000	-5.5120E-02	-6.6560E-02	-2.59E-02
Si	14000	-2.7037E-01	-3.0098E-01	-3.41E-01
S	16000	-2.3669E-03	-2.8035E-03	-3.08E-03
Cl	17000	-1.3000E-04	-3.0200E-05	-1.51E-04
K	19000	-1.9467E-02	-2.1899E-02	-1.28E-02
Ca	20000	-8.5427E-02	-6.6338E-02	-8.36E-002
Sc	21000	-3.4450E-06	-3.9660E-06	-4.75E-06
Ti	22000	-1.5900E-03	-1.7600E-03	-1.62E-03
Cr	24000	-9.4300E-05	-6.5710E-05	-1.10E-04
Fe	26000	-1.5870E-02	-1.5500E-20	-2.10E-02
Co	27000	-5.7810E-06	-5.5230E-06	-7.69E-06
Zn	30000	-1.0006E-04	-1.0680E-04	-6.57E-05
Rb	37000	-6.8500E-05	-8.6160E-05	-6.59E-05
Cs	55000	-1.9830E-06	-2.5860E-06	-1.10E-06
La	57000	-1.9965E-05	-1.5500E-02	-1.46E-05
Sm	62000	-1.5670E-06	-2.3780E-06	-2.25E-06
Eu	63000	-5.8510E-07	-6.9960E-07	-6.23E-07
Yb	70000	-1.0260E-06	-	-1.69E-06
W	74000	-7.5460E-05	-5.9570E-04	-1.75E-04
Th	90000	-4.3010E-06	-7.6160E-06	-6.10E-06

Neutron activation simulations

Simulations of concrete irradiation

Two different groups of simulations were carried out in this project with different purposes. The first aim was to create optimal material cards, which contain the important elements in terms of radiation protection, and to validate them by comparing simulated and measured data. For this purpose, models of the irradiation channels were constructed in MCNPX simulation code [19].

The constructed geometry consisted of the sample and the aluminium sample holder (see Figure 11 (a)) was placed in a 20×20×20 cm^3 cube, being a homogeneous volumetric neutron source. The experiments of both the Fast and Thermalized channels were reproduced in simulations with their typical neutron spectra which are presented in Figure 11 (b). The default spectral distributions of the channels were adjusted to the current measurements by scaling them with the measured flux parameters presented in Table 1.

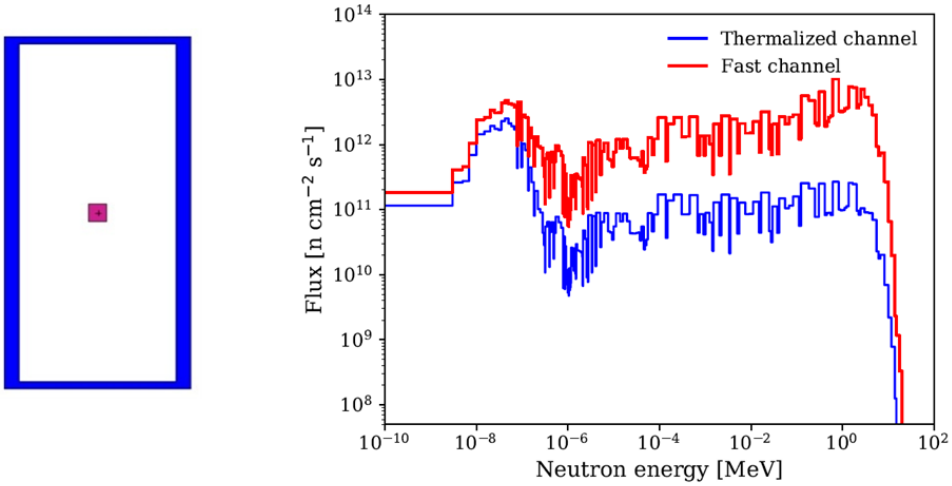

Figure 11 MCNP model for neutron irradiation simulations. (a) MCNP model for neutron irradiation in the vertical channels of the BRR. Pink: 5x5x5 mm^3 cube sample, blue: 4 mm thick cylindrical aluminium container. The sample holder is filled with void. (b) Typical neutron flux in the vertical channels of the BRR, scaled with measured flux parameters from the monitor foils.

Simulations were performed using these MCNPX output data and Cinder90 [20] with different initial compositions (i.e. 'material cards') for all three concretes: the nominal composition, the composition obtained from EDXRF and the composition based on the NAA and PGAA measurements. The results of the PGAA and the NAA methods were considered in combination, as they are practically complementary methods. The measurement-based compositions involved all elements indicated in

the nominal composition, extended with the parent elements of the 15 afore introduced key radioisotopes. Nominal values were applied non-detectable bulk elements. It is also important to note that the nominal composition based material cards contain similar elements to the currently available MCNP concrete material cards, like Los Alamos (MCNP) material card [27]. The simulated and measured activities were compared at t_0 time, which means right after irradiation, without cooling, in the times of the measurements, and also after 1 year- and 5 years of cooling. The 'measured data' of course were extrapolated for t_0, 1 y and 5 y.

The measured and simulated activity concentrations are compared in Figure 12 - Figure 14 for all three concretes. It is revealed that the simulations performed only with the nominal concrete composition highly underestimate the measured activities. The simulations gave only 0.1-28% and 10-41% of the measured activity for PE-B4C-concrete, and 0.2-20% and 12-28% for the Reference concrete in the Thermalized and Fast channels, respectively, due to the lack of trace elements. Trace elements, even in a couple ppm amounts can compose the majority of the activities of the samples as they can have several orders of magnitude higher neutron capture cross-sections than the bulk isotopes. This is further confirmed as the discrepancies between the simulated and measured results remarkably reduced with the application of either measurement-based initial composition. For all the concretes the first measured activity is consequently underestimated with all initial composition, understandably as the contribution of the key isotopes here is the lowest. Except of this data point, for the Thermalized channel (Figure 12 (a) - Figure 14 (a)) the discrepancies are in average within 40% based on either analytical method for most of the studied time period. Furthermore, the activities simulated with the recommended compositions agree with the measured data within 38% and 49% in the whole time period for the PE-B4C- and the Reference concrete, and within 16% and 23% without the consequently underestimated 4-day data points. In the case of EDXRF measurement based simulations, the activity after 5 years of cooling is underestimated with an order-of-magnitude, as it was shown that the main contributors to the activity at this time are the Co-60 and Eu-152, and none of their parent elements were measurable by the EDXRF method. The results of the Fast channel (Figure 12 (b) - Figure 14 (b)) are more varied, most likely due to the presence of threshold reactions and the resonance integral region, making the simulations particularly sensitive to the uncertainties of the irradiation neutron spectra. However, the activity simulations with the measured and recommended composition are considerably more realistic for these cases too, with at least 2 times higher activities than with the nominal composition. In essence, the activity increase due to the trace elements is comparable with the typical two- to three-fold safety reserve applied for Monte Carlo simulations.

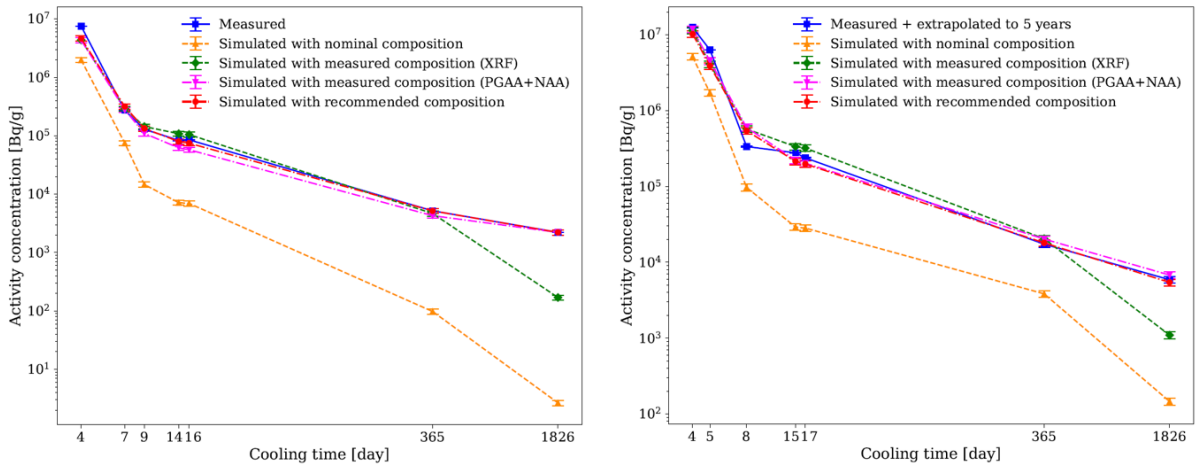

Figure 12 Measured decay profile of PE-B4C-concrete and simulated decay profiles with different initial compositions after irradiation in the Thermalized (a) and Fast channels (b). The statistical uncertainties are too small to be discernible. The measured points are connected for better visibility.

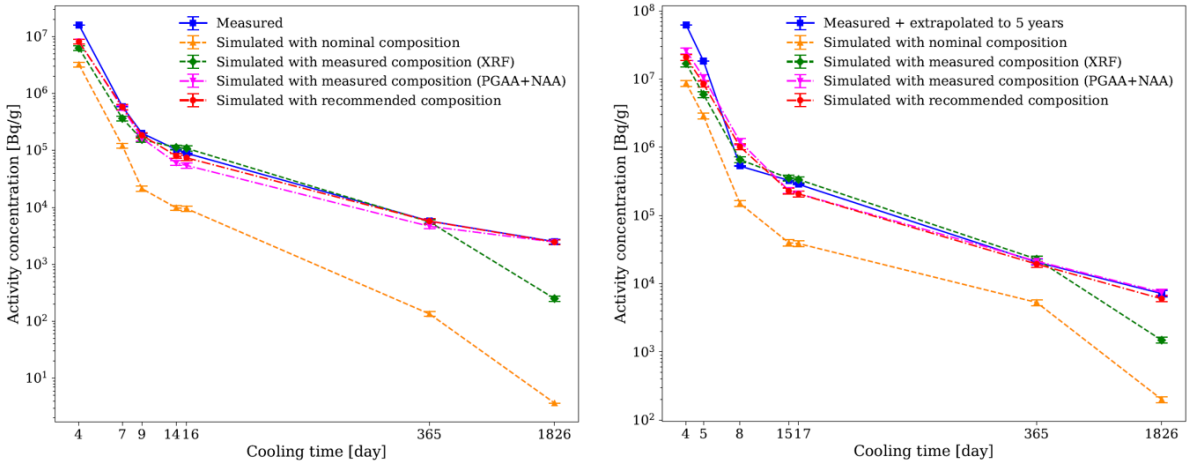

Figure 13 Measured decay profile of Reference concrete and simulated decay profiles with different initial compositions after irradiation in the Thermalized (a) and Fast channels (b). The statistical uncertainties are too small to be discernible. The measured points are connected for better visibility.

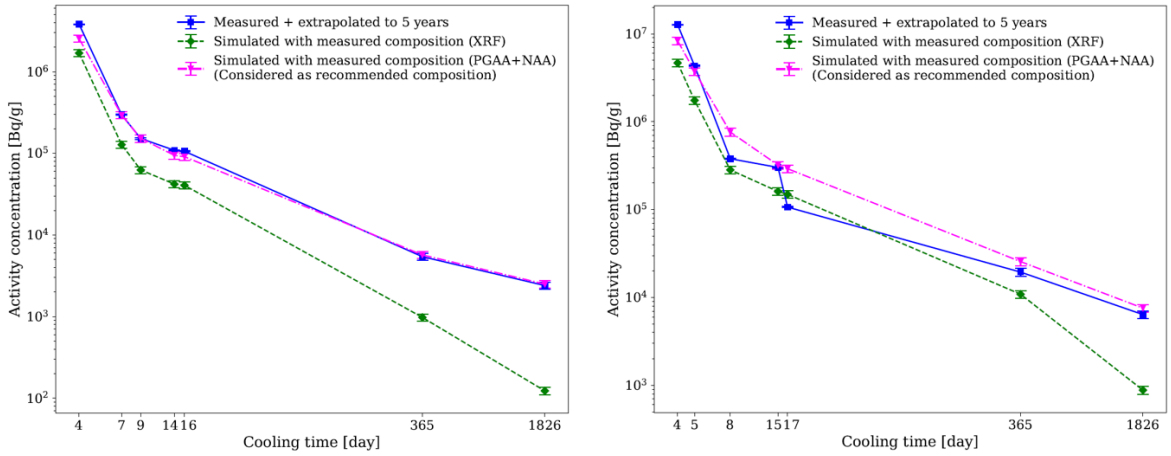

Figure 14 Measured decay profile of Skanska concrete and simulated decay profiles with different initial compositions after irradiation in the Thermalized (a) and Fast channels (b). The statistical uncertainties are too small to be discernible. The measured points are connected for better visibility.

Validation of recommended material cards

Additional irradiation simulations were performed for further validation of the `recommended compositions' of the PE-B4C- and the Reference concretes, determining the isotopic activities for the t_0 (end of irradiation time), and compared to the activities extrapolated from measured data for the same time. The results for the PE-B4C-concrete are presented and compared in Table 4. The activities agree within 15% for most isotopes. >50% differences were found for La-140 in the Thermalized irradiation channel and for Mn-54 and Yb-157 in the Fast channel. The case of La can be described as the La content was found to be very inhomogeneous among the samples, while Yb and Mn both have a resonance integrals in the high energy end of the applied neutron spectrum, being particularly sensitive for spectral uncertainties. These differences highlight the importance of extensive sampling for such inhomogeneous materials like concretes.

Table 4 Comparison of activity concentration measurement and simulation (with recommended composition) data in case of PE-B4C concrete for both Thermalized and Fast irradiation at t_0.

Isotope	Thermalized channel			Fast channel		
	Activity concentration [Bq/g]		Difference [%]	Activity concentration [Bq/g]		Difference [%]
	Measured	Simulated		Measured	Simulated	
Na-24	2.65E+08	3.53E+08	33	9.15E+08	7.59E+08	-17
W-187	4.51E+06	3.95E+06	-12	1.80E+07	1.51E+07	-16
La-140	3.90E+05	5.96E+05	53	1.46E+06	1.32E+06	-9
Sm-153	4.13E+05	3.06E+05	-26	1.92E+06	1.44E+06	-25
Yb-175	3.46E+04	2.40E+04	-31	1.08E+05	5.00E+04	-54
Rb-86	1.28E+04	1.50E+04	17	7.08E+04	7.02E+04	-1
Pa-233	4.45E+03	3.88E+03	-13	2.24E+04	1.60E+04	-29
Cr-51	3.16E+04	3.55E+04	12	7.60E+04	7.60E+04	0
Fe-59	1.75E+04	1.63E+04	-7	4.47E+04	3.77E+04	-16
Sc-46	1.71E+04	1.94E+04	13	4.61E+04	4.12E+04	-11
Zn-65	1.85E+03	1.87E+03	1	4.83E+03	4.76E+03	-1
Mn-54	2.69E+02	2.89E+02	7	8.53E+03	1.27E+04	49
Cs-134	6.06E+02	5.97E+02	-1	2.69E+03	2.49E+03	-7
Co-60	1.38E+03	1.41E+03	3	3.76E+03	3.47E+03	-8
Eu-152	1.60E+03	1.67E+03	5	4.35E+03	3.58E+03	-18

Simulations of ESS bunker

To evaluate the effect of trace elements on dose rate in a realistic case, the West Hall of the ESS bunker was used as a test case. The activation of two different concretes were studied, with in total three different initial compositions: the Reference concrete with its nominal and recommended compositions, and the compositions of normal concrete described in [28] that is currently used for bunker simulations in the ESS. To study the dose consequences of the concrete activation, an MCNP model was developed, describing the entire bunker complex according to present design (see Figure 15). As outlined in ESS-0416081: “Neutronic design of the bunker wall and roof” [28] the ESS bunker is assumed to be built from only two types of concrete: heavy concrete for the radial walls and roof and normal concrete for the axial wall. In order to have the most realistic setup for the simulations, the studied concrete was placed as the axial wall, and only this single wall was considered as source of decay gamma radiation, eliminating the effect of the surrounding heavy concrete shielding.

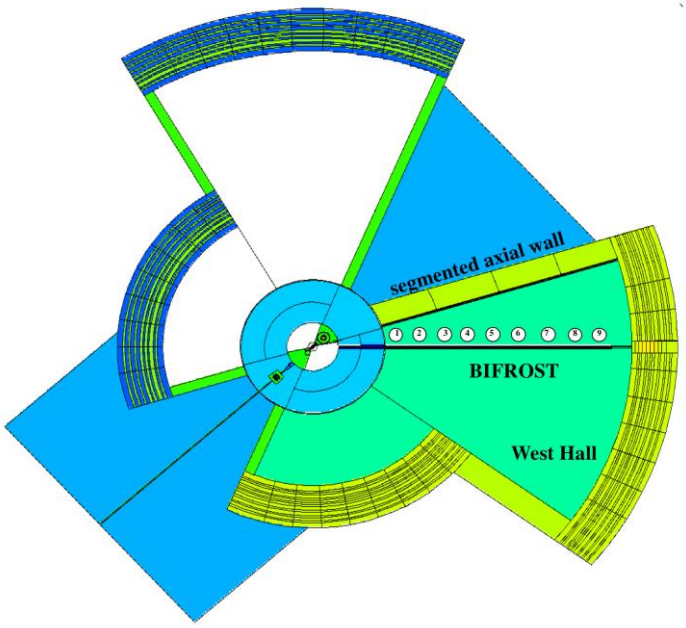

Figure 15 Overview of the MCNP model of the bunker complex. 1-9: 50 cm radius spheres along the neutron guide of the BIFROST instrument, marked areas for nominal comparison of decay-gamma dose rates.

The applied model includes the penetration through the monolith and guide segment corresponding to the BIFROST instrument in the West Hall. Tallies are prepared to measure neutron flux in the axial wall. To ensure accurate results, self-shielding is important to consider. In practice this means that the parts of the concrete facing the inside of the bunker are much more important for the dose in the bunker, than concrete behind it. For this purpose, the studied axial wall was divided into 36 segments as indicated in Figure 15. Decay gamma dose rates sourced by the activated isotopes of shielding concrete were simulated for a realistic, maintenance like irradiation scenario for the whole hall. In case of the simulations with the nominal and the recommended compositions of the Reference concrete the better comparison, gamma dose rates were quantified in 9 points with cylindrical tallies. Tallies were placed 2 meters from each other as it is indicated in Figure 15. Tallies are numbered from 1 to 9, where the first one is the closest to the source. The decay gamma dose rates were determined the following way:

1) MCNP transport simulation. The source is constituted by 2 GeV protons impinging on the tungsten target. The output is energy binned flux in segments of the radial wall on study, as well spallation induced isotope production rates. The results are normalized per initial proton.

2) In order to perform activation calculations, irradiation- and cooling scenarios were defined. In present analysis, we assume 10 years of ESS average operation (5 MW x 0.616), followed by 6 months of full power (5 MW) followed by 3 days of cooling.

3) Cinder activation calculation was carried out, based on steps 1)+2) and resulted in a characterization of the segment based production of radioisotopes. Using Gamma Script these data were used to define a corresponding Gamma source description.

4) Using the Gamma source provided in step 3) a second MCNP calculation was carried out, using the same geometry description as in Step 1), but transporting gammas and outputting the resulting fluxes on a spatial mesh, covering the region of interest, i.e. the West Hall. In case of the simulations of the nominal and recommended compositions of the Reference concrete, the dose rates were determined in addition for the 9 marked areas in Figure 15, selected for numerical comparison.

5) Finally, gamma fluxes were converted to doses, using energy depending conversion factors.

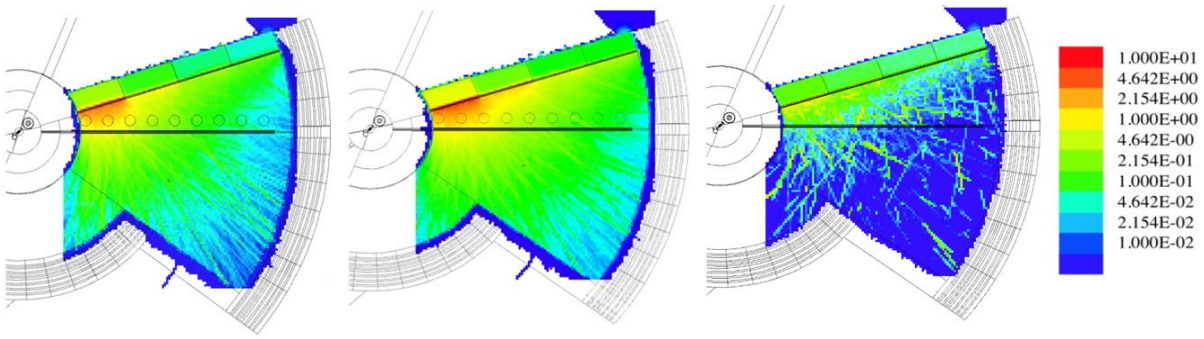

Figure 16 decay gamma dose rate maps $\left[\frac{\mu Sv}{h}\right]$ of the West Hall after 3 days of cooling, with different compositions of the axial wall: nominal composition of the Reference concrete in (a), recommended composition of the Reference concrete in (b) and the currently used concrete for bunker simulations given in [28]

The simulated decay gamma dose rates are presented inTable 5, and in Table 5. In Figure 16 it is demonstrated that in for the Reference concrete (Figure 16 (a), (b)), the dose rates significantly increase in the close proximity of the first quarter of the axial wall, and the area with $> 1 \frac{\mu Sv}{h}$ gamma dose rate (yellow) is also increased in the case of the recommended composition, compared to the nominal composition, due to the trace elements in one axial wall of the bunker. As the gamma dose rates for the Reference concrete are quite inhomogeneous in the bunker, the increase of dose rate in the selected areas varies between 29-72%, mostly increasing with the distance from the source, as presented in Table 5.

Table 5 Comparison of simulated dose rates in the West Hall of the ESS bunker with the recommended and nominal composition of the Reference concrete.

Tally number	Nominal composition		Recommended composition		Increase in dose rate [%]
	Dose rate [µSv/h]	Uncertainty [%]	Dose rate [µSv/h]	Uncertainty [%]	
1	1.89E+00	7.2	2.73E+00	5.8	45
2	1.79E+00	7.6	2.37E+00	6.2	33
3	9.37E-01	9.2	1.32E+00	6.7	41
4	4.99E-01	11.3	6.45E-01	7.1	29
5	2.52E-01	9.0	4.02E-01	6.9	59
6	1.87E-01	9.3	3.01E-01	6.7	61
7	1.24E-01	10.4	2.14E-01	7.9	72
8	7.75E-02	11.6	1.33E-01	8.3	72
9	6.07E-02	26.5	1.04E-01	16.7	71

In terms of the current ESS bunker shielding concrete, the simulated gamma dose rates are significantly, minimum an order of magnitude smaller than those for either composition of the Reference concrete. The main reason for this severe underestimation of the dose rates found to be the lack of Na in this concrete composition. As it was demonstrated, Na-24 is the dominant isotope in the first few days of cooling. It is worth mentioning that its main parent element, Na was indicated in the nominal composition of both PE-B4C- and the Reference concrete. This further confirms that a reliable input composition is essential for activation simulations. In addition, with the comparison of measured and nominal compositions of the Reference concrete it was also demonstrated that even with a realistic bulk composition, the presence or lack of trace elements in these simulations by themselves can multiple the simulated activities and decay gamma doses, approaching two-fold safety reserve of Monte Carlo dose simulations, required in the ESS [1].

Summary

A comprehensive study was carried out on the activation properties of neutron shielding concretes and metals of typical structural elements. Neutron activation of aluminium, stainless steel and copper, and that of three different concretes which were considered to be used at ESS were measured after irradiation in the Thermalized and Fast channels of the BRR.

It was found for all concrete samples, that Na-24 and W-187 are the dominant sources of activity in the first few days of cooling, while Co-60 and Eu-152 are giving the majority of the total activity in long-term, in accordance with the expectations. It was also demonstrated, that the activity concentration of the PE-B4C-concrete is significantly lower than that of the Reference concrete: 54% and 66% lower during the first week of cooling after being irradiated in the Thermalized and Fast channels, respectively. With this it is proven that the activation properties of the PE-B4C-concrete are more advantageous than that of the Reference concrete in terms of activation, especially during the first week of cooling, i.e. in a potential maintenance period. However, it was also shown that the decrease due to the added non-activating components is comparable to the activity variation due to different initial compositions, as the Skanska concrete found to be activated very similarly to the PE-B4C-concrete.

In order to take into account the activation products of shielding concretes more realistically in Monte Carlo simulations, the composition of all three concretes were determined with 3 analytical methods (NAA, PGAA and EDXRF). On the basis of the performed neutron activation measurements, the 15 most important gamma emitting radioisotopes - giving minimum 83% of the total measured activity for the whole studied time range - were identified, allowing a simple comparison of the measured and simulated activities. This simplification can be used in activation related safety considerations to evaluate both short- and long-term effects, not only in ESS, but in every neutron-emitting facilities (e.g. nuclear power plants). Activation simulations were performed with MCNP and Cinder90 codes for all the measured and nominal compositions (given by the manufacturer) of the 3 concretes. It was proven that the simulations with the nominal composition underestimate the measured activities with one order-of-magnitude, highlighting the importance of trace elements in terms of activation. On the basis of the measured composition, MCNP material cards were developed for the PE-B4C- and the Reference concretes that are recommended for activation calculations. Also for Skanska concrete, the composition measured with the combination of PGAA and NAA techniques is recommended for activation simulation purposes.

The importance of realistic material cards was also demonstrated in terms of radiation safety: decay gamma dose rates were calculated for a single concrete wall of the ESS West Hall with a realistic irradiation scenario for the Reference concrete and the current concrete composition used for bunker simulations in the ESS. It was found that after 3 days of cooling i.e. in maintenance period, the decay gamma dose rates simulated with the recommended, measurement-based material card of the Reference concrete resulted 29-72% higher dose rates than the nominal composition, which does not contain trace elements. Moreover, it was demonstrated, that the currently applied concrete composition severely underestimates the produced decay gamma dose rates, due to the lack of Na in the composition. This concrete produces one order-of-magnitude smaller dose rates than the Reference concrete even its nominal composition. This underlines that reliable input compositions are essential for activation simulations and that the presence of trace elements can multiple the simulated activities and decay gamma doses, approaching the two-fold conservative reserve of Monte Carlo safety simulations, required in the ESS.

To summarise, a detailed, comprehensive study was performed on the neutron activation properties of neutron shielding concretes and the measurement-based methodology was presented for the construction of detailed material cards for more realistic activation simulations.

Appendix A –

Measured activities and compositions of metal samples

Measured activities of metals

Table A 1 Aluminium sample irradiated in Thermalized channel. Gamma spectra were recorded four times.

Measurement		1		2		3		4	
Cooling time [d]		1		4		7		15	
Cooling time [s]		94513		364298		626516		1306151	
Isotope	$T_{1/2}$ [days]	A.c. [Bq/g]	*Unc. [%]*	A.c. [Bq/g]	*Unc. [%]*	A.c. [Bq/g]	*Unc. [%]*	A.c. [Bq/g]	*Unc. [%]*
Mn-56	**0.1**	2.51E+05	*1*					-	-
Ga-72	**0.6**	4.64E+04	*1*	1.02E+03	*2*	2.19E+01	*14*	-	-
Na-24	**0.6**	2.81E+04	*2*	8.13E+02	*2*	2.17E+01	*18*	-	-
La-140	**1.7**	3.03E+03	*13*	2.67E+02	*4*	7.53E+01	*4*	-	-
Sm-153	**1.9**	-	-	8.89E+01	*14*	3.66E+01	*15*	-	-
Np-239	**2.4**	-	-	4.16E+01	*20*	2.45E+01	*17*	-	-
Cr-51	**27.7**	-	-	2.87E+02	*17*	2.55E+02	*8*	2.28E+02	*6*
Hf-181	**42.4**	-	-	1.58E+01	*14*	1.43E+01	*8*	1.48E+01	*8*
Fe-59	**44.5**	-	-	5.67E+01	*13*	4.87E+01	*7*	5.83E+01	*8*
Sc-46	**83.8**	-	-	1.10E+01	*23*	-	-	1.07E+01	*7*
Zn-65	**244.3**	-	-	-	-	-	-	1.27E+01	*14*
Co-60	**1924**	-	-	-	-	1.65E+01	*14*	1.60E+01	*7*
Total*		**3.28E+05**		**2.60E+03**		**4.98E+02**		**3.24E+02**	

* Sum of the activity concentrations of the listed radioisotopes

Table A 2 Aluminium sample irradiated in the Fast channel. Gamma spectra were recorded five times.

Measurement		1		2		3		4		5	
Cooling time [d]		5		7		14		21		62	
Cooling time [s]		454173		625441		1227806		1844276		5329522.8	
Isotope	$T_{1/2}$ [days]	A.c. [Bq/g]	*Unc. [%]*	A.c. [Bq/g]	*Unc. [%]*	A.c. [Bq/g]	*Unc. [%]*	A.c. [Bq/g]	*Unc. [%]*	A.c. [Bq/g]	*Unc. [%]*
Ga-72	**0.6**	1.33E+04	*2*	8.98E+02	*9*	-	-	-	-	-	-
Na-24	**0.6**	8.86E+04	*1*	7.93E+03	*1*	-	-	-	-	-	-
As-76	**1.1**	8.62E+02	*16*	1.58E+02	*15*	-	-	-	-	-	-
La-140	**1.7**	6.46E+03	*2*	2.45E+03	*1*	1.73E+02	*2*	-	-	-	-
Sm-153	**1.9**	4.59E+03	*6*	2.16E+03	*6*	2.41E+02	*8*	2.88E+01	*17*	-	-
Np-239	**2.4**	3.27E+03	*6*	1.42E+03	*6*	2.33E+02	*3*	2.41E+01	*22*	-	-
Au-198	**2.7**	-	-	5.54E+01	*38*	1.75E+01	*24*	-	-	-	-
Sb-122	**2.7**	1.01E+03	*13*	4.86E+02	*9*	1.07E+02	*6*	1.70E+01	*43*	-	-
Mo-99[1]	**2.7**	3.46E+02	*19*	1.72E+02	*13*	3.58E+01	*7*	5.70E+00	*31*	-	-
Sc-47	**3.3**	2.96E+02	*23*	1.32E+02	*14*	3.65E+01	*15*	1.86E+01	*19*	-	-
Pa-233	**27**	-	-	-	-	7.61E+01	*15*	4.84E+01	*15*	-	-
Cr-51	**28**	1.00E+04	*11*	8.15E+03	*4*	7.50E+03	*2*	6.23E+03	*2*	2.27E+03	*1*
Ce-141	**33**	2.34E+02	*29*	5.43E+01	*32*	6.94E+01	*7*	5.63E+01	*9*	2.40E+01	*10*
Nb-95	**35**	-	-	-	-	1.51E+01	*30*	-	-	1.50E+01	*16*
Hf-181	**42**	5.76E+02	*10*	4.65E+02	*5*	5.03E+02	*1*	4.41E+02	*2*	2.29E+02	*1*
Fe-59	**45**	1.88E+03	*11*	1.56E+03	*5*	1.80E+03	*1*	1.64E+03	*1*	8.57E+02	*1*
Sb-124	**60**	7.09E+02	*20*	6.16E+01	*45*	6.41E+01	*4*	6.00E+01	*5*	3.92E+01	*4*
Zr-95	**64**	-	-	-	-	2.87E+01	*33*	0.00E+00	*24*	2.35E+01	*17*
Hf-175	**70**	-	-	4.78E+01	*25*	5.08E+01	*10*	5.92E+01	*8*	3.44E+01	*5*
Co-58	**71**	8.78E+02	*14*	6.32E+02	*5*	7.38E+02	*2*	6.80E+02	*1*	4.56E+02	*1*
Sc-46	**84**	4.14E+02	*25*	2.90E+02	*16*	3.66E+02	*1*	3.35E+02	*2*	2.37E+02	*1*
Ta-182	**114**	-	-	-	-	3.72E+01	*28*	-	-	-	-
Zn-65	**244**	-	-	-	-	4.39E+02	*3*	4.13E+02	*4*	3.73E+02	*3*
Co-60	**1924**	-	-	4.36E+02	*5*	5.85E+02	*2*	5.76E+02	*1*	5.75E+02	*1*
Eu-152	**4941**	-	-	-	-	-	-	-	-	1.63E+01	*26*
Total*		**1.33E+05**		**2.76E+04**		**1.31E+04**		**1.06E+04**		**5.15E+03**	

* Sum of the activity concentrations of the listed radioisotopes

[1] Mo-99 decays to Tc-99m, which has 6 h half-life, and emits a gamma photon with the same energy. Therefore, this value consists of the total activity concentration of the two isotopes

.

Table A 3 Copper sample irradiated in Thermalized channel. Gamma spectra were recorded three times.

Measurement		1		2		3	
Cooling time [d]		5.07		7.24		15	
Cooling time [s]		438104		625171		1298450	
Isotope	$T_{1/2}$ [days]	A.c. [Bq/g]	*Unc. [%]*	A.c. [Bq/g]	*Unc. [%]*	A.c. [Bq/g]	*Unc. [%]*
Cu-64	0.5	9.20E+06	*3*	3.55E+05	*3*	-	-
Ag-110m	249.8	-	-	5.81E+01	*27*	5.41E+01	*2*
Co-60[1]	1924.1	-	-	-	-	1.55E+01	*11*
Total*		9.20E+06		3.55E+05		6.96E+01	

* Sum of the activity concentrations of the listed radioisotopes

[1] Co-60 can be derived from Cu-63 as well, with (n,α) reaction induced by fast neutrons

Table A 4 Copper sample irradiated in Fast channel. Gamma spectra were recorded two times.

Measurement		1		2	
Cooling time [d]		14		22	
Cooling time [s]		1235143		1907382	
Isotope	$T_{1/2}$ [days]	A.c. [Bq/g]	*Unc. [%]*	A.c. [Bq/g]	*Unc. [%]*
Pb-203	2.2	1.99E+01	*27*	1.51E+01	*29*
Cu-67	2.6	2.89E+02	*4*	2.90E+01	*21*
Au-198	2.7	1.49E+02	*6*	-	-
Sb-122	2.7	3.70E+02	*4*	5.08E+01	*18*
Sb-124	60.2	2.57E+02	*3*	2.26E+02	*3*
Co-58	70.9	-	-	2.50E+01	*17*
Zn-65	244.3	1.73E+02	*17*	1.61E+02	*13*
Ag-110m	249.8	3.77E+03	*0.4*	3.65E+03	*0.5*
Co-60[1]	1924.1	7.24E+03	*1*	7.14E+03	*0.4*
Total*		1.23E+04		1.13E+04	

* Sum of the activity concentrations of the listed radioisotopes

[1] Co-60 can be derived from Cu-63 as well, with (n,α) reaction induced by fast neutrons

Table A 5 Stainless steel sample irradiated in Thermalized channel. Gamma spectra were recorded four times.

Measurement		1		2		3		4	
Cooling time [d]		1		4		7		16	
Cooling time [s]		93022		367728		628615		1400813	
Isotope	$T_{1/2}$ [days]	A.c. [Bq/g]	*Unc. [%]*	A.c. [Bq/g]	*Unc. [%]*	A.c. [Bq/g]	*Unc. [%]*	A.c. [Bq/g]	*Unc. [%]*
Mn-56	0.1	3.63E+06	*1*	-	-	-	-	-	-
Cu-64	0.5	1.75E+06	*30*	9.24E+03	*36*	-	-	-	-
As-76	1.1	1.58E+05	*5*	1.18E+04	*4*	2.29E+03	*12*	-	-
Sb-122	2.7	1.89E+04	*15*	3.76E+03	*5*	1.78E+03	*11*	-	-
Cr-51	27.7	1.74E+05	*13*	1.12E+05	*2*	1.02E+05	*2*	8.47E+04	*1*
Ce-141	32.5	-	-	5.68E+02	*20*	-	-	-	-
Fe-59	44.5	4.05E+05	*1*	1.98E+05	*1*	1.86E+05	*1*	1.64E+05	*1*
Sb-124	60.2	-	-	-	-	2.23E+02	*17*	1.81E+02	*14*
Mn-54	312.3	6.24E+04	*6*	2.85E+03	*9*	2.38E+03	*12*	2.63E+03	*5*
Co-60	1924.1	7.62E+03	*14*	4.05E+03	*2*	4.06E+03	*3*	4.11E+03	*1*
Total*		6.20E+06		3.42E+05		2.98E+05		2.55E+05	

* Sum of the activity concentrations of the listed radioisotopes

Table A 6 Stainless steel sample irradiated in Fast channel. Gamma spectra were recorded five times.

Measurement		1		2		3		4		5	
Cooling time [d]		5		7		14		21		64	
Cooling time [s]		455712		624069		1225512		1821653		5542066.8	
Isotope	$T_{1/2}$ [days]	A.c. [Bq/g]	*Unc. [%]*	A.c. [Bq/g]	*Unc. [%]*	A.c. [Bq/g]	*Unc. [%]*	A.c. [Bq/g]	*Unc. [%]*	A.c. [Bq/g]	*Unc. [%]*
As-76	1.1	7.04E+05	*3*	2.10E+05	*6*	-	-	-	-	-	-
Mo-99[1]	2.7	4.63E+04	*6*	2.57E+04	*11*	-	-	-	-	-	-
Sb-122	3	4.09E+05	*3*	2.43E+05	*4*	4.66E+04	*11*	-	-	-	-
Cr-51	28	6.14E+06	*2*	5.62E+06	*2*	4.41E+06	*1*	3.74E+06	*2*	1.07E+06	*2*
Fe-59	45	1.15E+07	*1*	1.08E+07	*0*	9.10E+06	*1*	7.98E+06	*1*	3.44E+06	*1*
Sb-124	60	2.81E+04	*9*	2.63E+04	*8*	2.03E+04	*6*	1.85E+04	*10*	-	-
Co-58	70.9	5.40E+04	*12*	6.18E+04	*9*	4.01E+04	*13*	4.16E+04	*10*	2.07E+04	*14*
Mn-54	312.3	2.61E+06	*1*	2.50E+06	*2*	2.31E+06	*1*	2.21E+06	*1*	1.70E+06	*1*
Co-60	1924.1	2.70E+05	*2*	2.59E+05	*2*	2.47E+05	*1*	2.36E+05	*1*	1.96E+05	*1*
Total*		2.18E+07		1.97E+07		1.62E+07		1.42E+07		6.42E+06	

* Sum of the activity concentrations of the listed radioisotopes

[1] Mo-99 decays to Tc-99m, which has 6 h half-life, and emits a gamma photon with the same energy. Therefore, this value consists of the total activity concentration of the two isotopes

Table A 7 Activity concentration of 'long' half -life radioisotopes in metal samples at t_0.

Isotope	$T_{1/2}$ [years]	Cu-[Bq/g]	S [Bq/g]	Al [Bq/g]
Zn-65	**0.67**	-	-	450
Ag-110m	**0.68**	3900	-	-
Mn-54	**0.86**	-	2200000	-
Co-60	**5.27**	7200	230000	590
Eu-152	**13.5**	-	-	20

Measured metal compositions

Table A 8 Comparison of measured composition of aluminium.

	Nominal	XRF	St.dev.	NAA	St.dev.
	[ppmw]				
Al	983000	970315	5697	-	-
Cr	2500	4385	2904	34.66	1.959
Cu	1000	-	-	26.28	1.995
Fe	5000	2198	356	2170	136.3
Ga	-	-	-	126.5	4.836
Hf	-	-	-	1.262	0.1015
La	-	-	-	1.994	0.09287
Mg	12000	9520	5108	-	-
Mn	10000	5909	1002	5212	191.3
Na	-	-	-	105.1	6.412
Si	13000	10239	716	-	-
Ti	1000	-	-	-	-
Zn	2000	-	-	32	6.121
Co	-	-	-	2.494	0.1932
V	-	100	40	-	-
Sc	-	-	-	0.09182	0.009952
Sm	-	-	-	0.05221	0.006714
U	-	-	-	0.599	0.07023

Table A 9 Comparison of measured composition of copper

	Nominal	XRF	St.dev.	NAA	St.dev.
	[ppmw]				
Ag	-	-	-	10.57	0.4028
Cu	999500	999379	361	834700	34010
Zn	-	690	423	4.038	0.8368
P	70	-	-	-	-
Bi	5	-	-	-	-
Pb	50	-	-	-	-
Co	-	-	-	0.7928	0.0388
Sb	-	-	-	0.157	0.02702

Table A 10 Comparison of measured composition of stainless steel

	Nominal	XRF	St.dev.	NAA	St.dev.
	[ppmw]				
Al	-	5370	1619	-	-
As	-	-	-	18.19	0.7358
Cr	4000	1858	68	1578	57.46
Cu	-	270	192	163.6	54.09
Fe	990000	987672	1864	862600	31100
Ga	-	-	-	15.3	0.7137
Mn	6500	6087	142	5521	199.3
Si	4000	2028	166	-	-
C	4600	-	-	-	-
Mo	1000	31	3	22.31	3.922
Ni	4000	-	-	-	-
S	-	160	65	-	-
Co	-	1190	602	76.78	2.901
Sn	-	100	51	-	-
Sb	-	-	-	3.649	0.2018

Appendix B –

Measured activities of concrete samples

Table B 1 PE-B4C sample irradiated in Thermalized channel. Gamma spectra were recorded five times.

Measurement		1		2		3		4		5	
Isotope	**$T_{1/2}$ [days]**	**A.c. [Bq/g]**	***Unc. [%]***	**A.c. [Bq/g]**	***Unc. [%]***	**A.c. [Bq/g]**	***Unc. [%]***	**A.c. [Bq/g]**	***Unc. [%]***	**A.c. [Bq/g]**	***Unc. [%]***
K-42	**0.5**	3.80E+05	*15*	-	-	-	-	-	-	-	-
Na-24	**0.6**	6.45E+06	*1*	1.05E+05	*1*	1.07E+04	*2*	-	-	-	-
W-187	**1.0**	4.32E+05	*3*	3.25E+04	*3*	7.53E+03	*4*	3.62E+02	*26*	-	-
As-76	**1.1**	-	-	2.30E+03	*17*	-	-	-	-	-	-
La-140	**1.7**	1.15E+05	*4*	1.95E+04	*2*	8.43E+03	*1*	1.30E+03	*3*	6.89E+02	*4*
Sm-153	**1.9**	1.29E+05	*8*	3.12E+04	*5*	1.52E+04	*4*	2.75E+03	*6*	1.66E+03	*6*
Np-239[1]	**2.4**	-	-	3.34E+03	*20*	1.49E+03	*15*	4.13E+02	*15*	2.20E+02	*26*
Sb-122	**2.7**	-	-	2.68E+03	*14*	1.69E+03	*7*	5.34E+02	*17*	3.76E+02	*19*
Sc-47[2]	**3.3**	-	-	3.38E+03	*7*	3.03E+03	*3*	1.85E+03	*4*	1.76E+03	*3*
Yb-175	**4.2**	-	-	1.37E+04	*25*	8.15E+03	*21*	3.11E+03	*25*	3.25E+03	*14*
Ca-47	**4.5**	-	-	2.08E+03	*17*	1.61E+03	*11*	9.49E+02	*5*	7.62E+02	*12*
Lu-177	**6.7**	-	-	5.23E+03	*22*	3.11E+03	*15*	1.93E+03	*15*	1.79E+03	*12*
Ba-131	**12**	-	-	9.86E+02	*10*	1.57E+03	*4*	1.40E+03	*4*	1.22E+03	*4*
Rb-86	**19**	-	-	-	-	1.01E+04	*18*	6.91E+03	*20*	7.69E+03	*10*
Pa-233[3]	**27**	-	-	9.65E+02	*12*	2.89E+03	*7*	2.82E+03	*5*	3.21E+03	*4*
Cr-51	**28**	-	-	2.18E+04	*10*	2.09E+04	*6*	2.16E+04	*3*	2.17E+04	*2*
Yb-169	**32**	-	-	-	-	3.82E+02	*29*	4.36E+02	*15*	4.76E+02	*14*
Ce-141	**33**	-	-	1.69E+03	*11*	1.73E+03	*8*	1.74E+03	*4*	1.99E+03	*3*
Hf-181	**42**	-	-			8.03E+02	*8*	9.02E+02	*4*	1.05E+03	*3*
Fe-59	**45**	-	-	1.13E+04	*4*	1.21E+04	*2*	1.34E+04	*1*	1.42E+04	*2*
Sb-124	**60**	-	-	-	-	-	-	2.69E+02	*6*	3.43E+02	*6*
Sr-85	**65**	-	-	-	-	-	-	1.56E+02	*23*	2.12E+02	*26*
Tb-160	**72**	-	-	-	-	-	-	5.56E+02	*16*	6.11E+02	*10*
Sc-46[4]	**84**	2.22E+04	*23*	1.30E+04	*2*	1.26E+04	*2*	1.44E+04	*1*	1.58E+04	*1*
Ta-182	**114**	-	-	-	-	0.00E+00	*0*	5.01E+02	*22*	3.83E+02	*22*
Zn-65	**244**	-	-	1.57E+03	*24*	1.35E+03	*13*	1.65E+03	*7*	1.90E+03	*6*
Mn-54[5]	**312**	-	-	-	-	-	-	2.96E+02	*25*	2.25E+02	*25*
Cs-134	**754**	-	-	-	-	4.49E+02	*12*	5.90E+02	*6*	6.06E+02	*5*
Co-60	**1924**	-	-	1.14E+03	*16*	1.15E+03	*6*	1.31E+03	*2*	1.43E+03	*3*
Eu-152	**4941**	-	-	-	-	1.58E+03	*7*	1.46E+03	*4*	1.74E+03	*2*
Total*		**7.53E+06**		**2.73E+05**		**1.29E+05**		**8.37E+04**		**8.52E+04**	

* Sum of the activity concentrations of the listed radioisotopes

Table B 2 Reference concrete sample irradiated in Thermalized channel. Gamma spectra were recorded five times.

Measurement		1		2		3		4		5	
Isotope	$T_{1/2}$ [days]	A.c. [Bq/g]	*Unc. [%]*	A.c. [Bq/g]	*Unc. [%]*	A.c. [Bq/g]	*Unc. [%]*	A.c. [Bq/g]	*Unc. [%]*	A.c. [Bq/g]	*Unc. [%]*
K-42	**0.5**	5.23E+05	*11*	4.77E+03	*25*	-	-	-	-	-	-
Na-24	**0.6**	1.18E+07	*1*	1.82E+05	*1*	1.61E+04	*2*	-	-	-	-
W-187	**1.0**	3.77E+06	*1*	2.54E+05	*1*	5.53E+04	*1*	1.82E+03	*6*	4.60E+02	*21*
As-76	**1.1**	-	-	1.57E+03	*26*	6.23E+02	*21*	-	-	-	-
La-140	**1.7**	2.14E+05	*3*	3.32E+04	*1*	1.34E+04	*1*	2.08E+03	*3*	9.99E+02	*3*
Sm-153	**1.9**	2.22E+05	*5*	4.93E+04	*4*	2.24E+04	*3*	4.34E+03	*4*	2.06E+03	*6*
Np-239	**2.4**	-	-	5.94E+03	*12*	1.86E+03	*14*	5.82E+02	*18*	3.25E+02	*25*
Sb-122	**2.7**	-	-	2.80E+03	*12*	1.54E+03	*9*	5.32E+02	*21*	3.29E+02	*19*
Sc-47	**3.3**	-	-	4.22E+03	*10*	2.95E+03	*6*	2.04E+03	*4*	1.53E+03	*5*
Yb-175	**4.2**	-	-	-	-	9.44E+03	*21*	5.02E+03	*14*	3.22E+03	*20*
Ca-47	**4.5**	-	-	2.04E+03	*13*	1.86E+03	*13*	1.08E+03	*10*	6.99E+02	*11*
Lu-177	**6.7**	-	-	-	-	3.54E+03	*24*	2.72E+03	*11*	2.28E+03	*10*
Ba-131	**12**	-	-	2.39E+03	*12*	2.26E+03	*5*	1.94E+03	*3*	1.62E+03	*3*
Rb-86	**19**	-	-	-	-	1.12E+04	*14*	1.09E+04	*11*	1.01E+04	*9*
Pa-233	**27**	-	-	-	-	6.08E+03	*9*	5.96E+03	*4*	5.43E+03	*3*
Cr-51	**28**	-	-	1.70E+04	*22*	1.49E+04	*9*	1.67E+04	*2*	1.55E+04	*5*
Yb-169	**32**	-	-	-	-	-	-	6.15E+02	*14*	5.12E+02	*11*
Ce-141	**33**	-	-	3.08E+03	*12*	3.23E+03	*7*	3.02E+03	*4*	2.79E+03	*3*
Hf-181	**42**	-	-	1.34E+03	*21*	1.07E+03	*13*	1.15E+03	*6*	1.16E+03	*4*
Fe-59	**45**	-	-	1.34E+04	*4*	1.27E+04	*3*	1.53E+04	*1*	1.39E+04	*1*
Sb-124	**60**	-	-	-	-	-	-	3.13E+02	*7*	2.49E+02	*14*
Sr-85	**65**	-	-	-	-	-	-	2.47E+02	*18*	3.16E+02	*19*
Tb-160	**72**	-	-	-	-	-	-	7.03E+02	*18*	7.12E+02	*9*
Sc-46	**84**	-	-	1.67E+04	*2*	1.59E+04	*2*	1.94E+04	*1*	1.82E+04	*1*
Ta-182	**114**	-	-	-	-	-	-	6.97E+02	*14*	5.67E+02	*11*
Zn-65	**244**	-	-	-	-	1.36E+03	*25*	1.95E+03	*9*	1.79E+03	*13*
Mn-54	**312**	-	-	-	-	-	-	-	-	2.80E+02	*22*
Cs-134	**754**	-	-	-	-	7.11E+02	*15*	7.29E+02	*5*	7.78E+02	*5*
Co-60	**1924**	-	-	1.30E+03	*13*	1.09E+03	*10*	1.54E+03	*3*	1.42E+03	*2*
Eu-152	**4941**	-	-	-	-	1.73E+03	*9*	2.33E+03	*4*	2.07E+03	*3*
Total*		**1.60E+07**		**5.89E+05**		**2.01E+05**		**1.04E+05**		**8.93E+04**	

* Sum of the activity concentrations of the listed radioisotopes

Table B 3 Reference concrete sample irradiated in Fast channel. Gamma spectra were recorded five times.

Measurement		1		2		3		4		5	
Isotope	**$T_{1/2}$ [days]**	**A.c. [Bq/g]**	***Unc. [%]***	**A.c. [Bq/g]**	***Unc. [%]***	**A.c. [Bq/g]**	***Unc. [%]***	**A.c. [Bq/g]**	***Unc. [%]***	**A.c. [Bq/g]**	***Unc. [%]***
K-42	**0.5**	1.93E+06	*9*	3.41E+05	*15*	-	-	-	-	-	-
Na-24	**0.6**	3.77E+07	*1*	9.18E+06	*1*	1.56E+04	*2*	-	-	-	-
W-187	**1.0**	2.04E+07	*1*	7.62E+06	*1*	1.23E+05	*1*	4.63E+03	*5*	-	-
As-76	**1.1**	1.79E+05	*14*	7.53E+04	*17*	1.02E+03	*27*	-	-	-	-
La-140	**1.7**	7.25E+05	*2*	3.55E+05	*2*	2.42E+04	*1*	3.93E+03	*2*	1.68E+03	*3*
Sm-153	**1.9**	1.17E+06	*3*	6.02E+05	*4*	6.63E+04	*3*	1.40E+04	*4*	6.26E+03	*5*
Np-239	**2.4**	-	-	-	-	1.05E+04	*10*	2.74E+03	*15*	1.22E+03	*19*
Sb-122	**2.7**	9.16E+04	*16*	4.34E+04	*17*	7.46E+03	*6*	2.91E+03	*8*	1.47E+03	*10*
Sc-47	**3.3**	-	-	2.44E+04	*18*	9.17E+03	*4*	5.97E+03	*2*	4.24E+03	*3*
Yb-175	**4.2**	-	-	-	-	2.07E+04	*12*	1.01E+04	*10*	6.72E+03	*14*
Ca-47	**4.5**	-	-	-	-	3.41E+03	*11*	1.98E+03	*10*	1.51E+03	*6*
Lu-177	**6.7**	-	-	-	-	9.27E+03	*19*	6.40E+03	*11*	4.70E+03	*10*
Ba-131	**12**	-	-	-	-	1.11E+04	*2*	9.95E+03	*1*	8.54E+03	*1*
Rb-86	**19**	-	-	-	-	5.10E+04	*5*	5.33E+04	*2*	4.84E+04	*5*
Pa-233	**27**	-	-	6.10E+04	*22*	2.35E+04	*4*	2.49E+04	*2*	2.38E+04	*2*
Cr-51	**28**	-	-	-	-	4.14E+04	*6*	4.73E+04	*3*	4.33E+04	*2*
Yb-169	**32**	-	-	-	-	2.14E+03	*20*	1.77E+03	*15*	1.79E+03	*12*
Ce-141	**33**	-	-	-	-	7.05E+03	*6*	7.38E+03	*3*	7.05E+03	*2*
Hf-181	**42**	-	-	-	-	3.48E+03	*8*	3.50E+03	*5*	3.55E+03	*2*
Fe-59	**45**	-	-	-	-	3.08E+04	*2*	3.92E+04	*1*	3.69E+04	*1*
Sb-124	**60**	-	-	-	-	1.51E+03	*6*	1.85E+03	*2*	1.83E+03	*3*
Zr-95	**64**	-	-	-	-	-	-	8.88E+02	*11*	7.57E+02	*22*
Sr-85	**65**	-	-	-	-	1.07E+03	*17*	1.33E+03	*7*	1.06E+03	*9*
Co-58	**71**	-	-	-	-	5.61E+02	*20*	4.23E+02	*24*	5.93E+02	*18*
Tb-160	**72**	-	-	-	-	3.30E+03	*9*	3.31E+03	*4*	3.34E+03	*6*
Sc-46	**84**	1.01E+05	*20*	8.45E+04	*7*	3.87E+04	*1*	4.81E+04	*1*	4.69E+04	*1*
Ta-182	**114**	-	-	0.00E+00	*0*	3.10E+03	*19*	4.32E+03	*3*	4.11E+03	*3*
Zn-65	**244**	-	-	-	-	3.40E+03	*11*	4.84E+03	*5*	5.03E+03	*6*
Mn-54	**312**	-	-	-	-	6.85E+03	*5*	8.87E+03	*3*	8.85E+03	*3*
Cs-134	**754**	-	-	-	-	2.79E+03	*5*	3.44E+03	*2*	3.38E+03	*2*
Co-60	**1924**	-	-	-	-	2.89E+03	*3*	3.98E+03	*2*	3.86E+03	*1*
Eu-152	**4941**	-	-	-	-	4.63E+03	*6*	5.67E+03	*3*	5.58E+03	*2*
Total*		**6.04E+07**		**1.80E+07**		**5.30E+05**		**3.27E+05**		**2.86E+05**	

* Sum of the activity concentrations of the listed radioisotopes

Table B 4 Skanska concrete sample irradiated in Thermalized channel. Gamma spectra were recorded five times.

Measurement		1		2		3		4		5	
Isotope	**$T_{1/2}$ [days]**	**A.c. [Bq/g]**	***Unc. [%]***	**A.c. [Bq/g]**	***Unc. [%]***	**A.c. [Bq/g]**	***Unc. [%]***	**A.c. [Bq/g]**	***Unc. [%]***	**A.c. [Bq/g]**	***Unc. [%]***
K-42	**0.5**	2.65E+05	*8*	2.42E+03	*28*	-	-	-	-	-	-
Na-24	**0.6**	2.43E+06	*1*	4.60E+04	*1*	4.16E+03	*3*	-	-	-	-
W-187	**1.0**	7.95E+05	*3*	7.23E+04	*2*	1.50E+04	*2*	4.47E+02	*23*	-	-
As-76	**1.1**	2.04E+04	*27*	2.32E+03	*15*	-	-	-	-	-	-
La-140	**1.7**	1.08E+05	*3*	2.15E+04	*1*	9.13E+03	*1*	1.16E+03	*3*	6.61E+02	*4*
Sm-153	**1.9**	1.39E+05	*6*	3.98E+04	*4*	1.84E+04	*4*	2.82E+03	*6*	1.87E+03	*6*
Np-239	**2.4**	-	-	2.19E+03	*29*	9.34E+02	*28*	-	-	-	-
Sb-122	**2.7**	8.57E+03	*29*	3.07E+03	*11*	1.49E+03	*11*	4.21E+02	*18*	3.60E+02	*20*
Sc-47	**3.3**	-	-	3.98E+03	*4*	3.13E+03	*3*	2.28E+03	*2*	1.98E+03	*3*
Yb-175	**4.2**	-	-	1.92E+04	*11*	1.26E+04	*21*	5.13E+03	*18*	5.76E+03	*10*
Ca-47	**4.5**	-	-	2.75E+03	*14*	1.87E+03	*10*	1.06E+03	*10*	9.48E+02	*7*
Lu-177	**6.7**	-	-	6.15E+03	*18*	4.57E+03	*18*	3.67E+03	*10*	3.30E+03	*8*
Ba-131	**12**	-	-	2.15E+03	*11*	1.45E+03	*7*	1.28E+03	*3*	1.09E+03	*4*
Rb-86	**19**	-	-			8.07E+03	*14*	8.01E+03	*8*	7.90E+03	*7*
Pa-233	**27**	-	-	5.21E+03	*8*	4.18E+03	*7*	4.45E+03	*4*	4.26E+03	*4*
Cr-51	**28**	-	-	2.50E+04	*12*	2.46E+04	*4*	2.53E+04	*3*	2.54E+04	*3*
Yb-169	**32**	-	-			6.83E+02	*24*	6.56E+02	*13*	6.68E+02	*15*
Ce-141	**33**	-	-	2.66E+03	*9*	2.29E+03	*7*	2.43E+03	*3*	2.40E+03	*4*
Hf-181	**42**	-	-	1.72E+03	*11*	1.71E+03	*6*	1.88E+03	*3*	1.77E+03	*3*
Fe-59	**45**	2.63E+04	*18*	1.68E+04	*3*	1.58E+04	*2*	1.96E+04	*1*	1.92E+04	*1*
Sb-124	**60**	-	-	-	-	-	-	3.36E+02	*6*	3.62E+02	*7*
Tb-160	**72**	-	-	-	-	-	-	8.03E+02	*11*	8.86E+02	*12*
Sc-46	**84**	-	-	1.88E+04	*1*	1.74E+04	*1*	2.20E+04	*1*	2.16E+04	*1*
Ta-182	**114**	-	-	-	-	-	-	4.27E+02	*22*	4.08E+02	*14*
Zn-65	**244**	-	-	9.80E+02	*30*	8.86E+02	*16*	1.15E+03	*11*	1.15E+03	*8*
Cs-134	**754**	-	-	-	-	-	-	3.74E+02	*8*	3.66E+02	*9*
Co-60	**1924**	-	-	1.60E+03	*7*	1.56E+03	*4*	2.04E+03	*2*	1.98E+03	*2*
Eu-152	**4941**	-	-	-	-	1.64E+03	*5*	1.62E+03	*3*	1.67E+03	*4*
Total*		**3.82E+06**		**2.97E+05**		**1.52E+05**		**1.09E+05**		**1.06E+05**	

* Sum of the activity concentrations of the listed radioisotopes

Table B 5 Skanska concrete sample irradiated in Thermalized channel. Gamma spectra were recorded four times.

Measurement		1		2		3		4	
Isotope	**$T_{1/2}$ [days]**	**A.c. [Bq/g]**	***Unc. [%]***	**A.c. [Bq/g]**	***Unc. [%]***	**A.c. [Bq/g]**	***Unc. [%]***	**A.c. [Bq/g]**	***Unc. [%]***
K-42	**0.5**	8.29E+05	*11*	2.14E+05	*27*	-	-	-	-
Na-24	**0.6**	6.96E+06	*1*	1.83E+06	*1*	4.18E+03	*4*	-	-
W-187	**1.0**	3.73E+06	*2*	1.54E+06	*1*	3.47E+04	*2*	1.43E+03	*12*
As-76	**1.1**	1.16E+05	*10*	5.74E+04	*11*	1.61E+03	*13*	-	-
La-140	**1.7**	2.68E+05	*2*	1.41E+05	*2*	1.28E+04	*2*	2.28E+03	*3*
Sm-153	**1.9**	5.80E+05	*5*	3.29E+05	*4*	4.62E+04	*3*	9.55E+03	*4*
Np-239	**2.4**	-	-	-	-	3.00E+03	*17*	1.05E+03	*20*
Sb-122	**2.7**	6.26E+04	*12*	3.30E+04	*11*	6.93E+03	*6*	2.22E+03	*7*
Sc-47	**3.3**	-	-	2.65E+04	*15*	1.02E+04	*3*	6.80E+03	*2*
Yb-175	**4.2**	-	-	-	-	2.38E+04	*10*	1.02E+04	*11*
Ca-47	**4.5**	-	-	1.49E+04	*26*	4.41E+03	*7*	2.72E+03	*6*
Lu-177	**6.7**	-	-	-	-	1.13E+04	*10*	8.09E+03	*7*
Ba-131	**12**	-	-	-	-	6.66E+03	*4*	5.99E+03	*2*
Rb-86	**19**	-	-	-	-	3.38E+04	*13*	3.85E+04	*5*
Pa-233	**27**	-	-	-	-	1.01E+04	*5*	1.05E+04	*4*
Cr-51	**28**	-	-	-	-	5.41E+04	*4*	5.61E+04	*3*
Yb-169	**32**	-	-	-	-	1.98E+03	*17*	2.21E+03	*9*
Ce-141	**33**	-	-			4.82E+03	*6*	4.90E+03	*4*
Hf-181	**42**	-	-	8.15E+03	*18*	3.82E+03	*7*	4.58E+03	*2*
Fe-59	**45**	8.43E+04	*20*	5.23E+04	*9*	3.78E+04	*1*	4.74E+04	*1*
Sb-124	**60**	-	-	-	-	1.19E+03	*12*	2.00E+03	*5*
Zr-95	**64**	-	-	-	-	-	-	8.84E+02	*22*
Sr-85	**65**	-	-	-	-	-	-	5.38E+02	*17*
Co-58	**71**	-	-	-	-	-	-	7.33E+02	*20*
Tb-160	**72**	-	-	-	-	2.68E+03	*7*	3.37E+03	*7*
Sc-46	**84**	7.96E+04	*11*	6.40E+04	*6*	4.19E+04	*1*	5.22E+04	*1*
Ta-182	**114**	-	-	-	-	1.88E+03	*17*	2.48E+03	*6*
Zn-65	**244**	-	-	-	-	2.52E+03	*12*	3.43E+03	*8*
Mn-54	**312**	-	-	1.32E+04	*28*	8.29E+03	*6*	1.07E+04	*3*
Cs-134	**754**	-	-	-	-	1.05E+03	*12*	1.54E+03	*6*
Co-60	**1924**	-	-	-	-	3.58E+03	*3*	4.90E+03	*2*
Eu-152	**4941**	-	-	-	-	3.87E+03	*4*	4.29E+03	*3*
Total*		**1.27E+07**		**4.32E+06**		**3.79E+05**		**3.01E+05**	

* Sum of the activity concentrations of the listed radioisotopes

Appendix C – Measured compositions of concrete samples

Table C 1 Measured and nominal composition of PE-B4C-concrete.

		[w%]					
Element	**Nominal**	**PGAA**	**Unc. %**	**XRF**	**Unc. %**	**NAA**	**Unc. %**
H	2.31	1.26	3.2	-	-	-	-
C	8.99	5.46	11.9	-	-	-	-
Na	0.62	1.11	4.2	1.29	15.2	1.21	3.7
Al	2.35	3.44	3.7	5.51	0.6	-	-
Si	28.60	21.50	3.3	27.04	0.0	-	-
S	0.28	0.23	5.5	0.24	6.5	-	-
K	1.26	1.39	3.7	1.95	0.0	-	-
Ca	8.10	6.50	3.9	8.54	0.0	-	-
Fe	0.84	1.12	1.6	1.47	0.0	1.59	4.6
B	0.6	0.2	20.0	-	-	-	-
O	45.80	56.35	0.0	-	-	-	-
				[ppmw]			
Mg	1960	-	-	982.57	30.0	-	-
Ti	521.00	1030.00	1.7	1590.00	0.6	-	-
P	260	-	-	-	-	-	-
Cl	36	156.0	2.7	130.00	7.7	-	-
V	-	77.0	6.0	57.62	12.3	-	-
Sm	-	1.5	6.0	-	-	1.57	4.1
Gd	-	1.6	10.0	-	-	-	-
Mn	-	-	-	230.00	4.3	-	-
Sc	-	-	-	11.76	29.0	3.45	3.7
Cr	-	-	-	82.18	1.6	94.30	4.0
Co	-	-	-	-	-	5.78	4.3
Ni	-	-	-	11.68	6.7	-	-
Cu	-	-	-	43.53	1.5	-	-
Zn	-	-	-	100.06	0.9	107.70	5.8
Ga	-	-	-	7.84	5.5	-	-
Ge	-	-	-	4.87	5.8	-	-
As	-	-	-	2.92	4.9	-	-
Rb	-	-	-	59.36	0.7	68.50	7.1
Sr	-	-	-	311.67	0.4	-	-
Y	-	-	-	11.55	1.7	-	-
Zr	-	-	-	91.43	0.4	-	-
Nb	-	-	-	5.36	2.5	-	-
Mo	-	-	-	3.03	4.3	-	-
In	-	-	-	1.70	11.4	-	-
Sn	-	-	-	2.81	1.7	-	-
Sb	-	-	-	1.59	14.4	1.43	8.9
Cs	-	-	-	2.58	11.7	1.98	6.5
Ba	-	-	-	508.51	0.2	514.20	4.9
La	-	-	-	19.97	1.4	12.97	4.0
Ce	-	-	-	41.16	1.3	31.35	4.2
Pr	-	-	-	4.84	9.5	-	-
Nd	-	-	-	19.55	1.1	14.15	10.0
W	-	-	-	--	-	75.46	4.1
Pb	-	-	-	18.31	4.7	-	-
Th	-	-	-	3.85	7.8	4.30	4.3
U	-	-	-	2.70	13.6	-	-
Eu	-	-	-	-	-	0.59	4.4
Hf	-	-	-	-	-	2.70	4.6
Tb	-	-	-	-	-	0.30	11.7
Yb	-	-	-	-	-	1.03	9.3

Table C 2 Measured and nominal composition of Reference concrete.

		[w%]					
Element	**Nominal**	**PGAA**	**Unc. %**	**XRF**	**Unc. %**	**NAA**	**Unc. %**
H	0.72	0.60	1.6	-	-	-	-
C	-	-	-	-	-	-	-
Na	1.06	2.00	2.4	1.97	10.0	1.99	3.7
Al	3.70	5.29	2.2	6.66	0.5	-	-
Si	32.70	31.32	0.8	30.10	0.0	-	-
S	0.24	0.28	3.8	-	-	-	-
K	2.12	2.13	2.2	2.19	0.0	-	-
Ca	7.12	7.08	2.8	6.63	0.0	-	-
Ti	0.09	0.16	2.5	0.18	0.6	-	-
Mn	-	0.03	3.5	0.02	4.3	-	-
Fe	1.16	1.36	2.6	1.34	0.0	1.55	3.8
O	50.80	50.24	-	-	-	-	-
				[ppmw]			
B		24.90	1.2	-	-	-	-
Cl	30	169.00		-	-	-	-
V	-	70.00	7.0	55.53	0.4		
Sm	-	1.97	1.8	-	-	2.38	4.1
Gd	-	2.20	6.0	-	-	-	-
Mg	2370	-	-	9530.16	31.0	-	-
Sc	-	-	-	14.27	14.9	3.97	3.6
Cr	-	-	-	44.31	0.7	65.71	4.2
Co	-	-	-	-	-	5.52	4.4
Ni	-	-	-	6.40	-	-	-
Cu	-	-	-	22.43	2.1	-	-
Zn	-	-	-	87.67	0.5	106.80	6.0
Ga	-	-	-	10.92	5.7	-	-
Ge	-	-	-	3.20	7.1	-	-
As	-	-	-	-	-	-	-
Rb	-	-	-	75.97	1.0	86.16	6.4
Sr	-	-	-	380.93	0.4	-	-
Y	-	-	-	12.35	3.4	-	-
Zr	-	-	-	114.14	0.7	-	-
Nb	-	-	-	6.20	1.0	-	-
Mo	-	-	-	2.18	3.9	-	-
In	-	-	-	1.28	5.1	-	-
Sn	-	-	-	2.81	10.8	-	-
Sb	-	-	-	1.25	12.4	1.25	7.9
Cs	-	-	-	3.95	1.6	2.59	7.8
Ba	-	-	-	665.15	0.2	640.70	4.7
La	-	-	-	23.72	1.2	21.44	3.9
Ce	-	-	-	37.03	21.3	45.75	4.0
Pr	-	-	-	5.49	10.0	-	-
Nd	-	-	-	18.60	23.1	20.32	8.0
W	-	-	-	-	-	595.70	3.6
Pb	-	-	-	19.40	1.9	-	-
Th	-	-	-	4.71	4.9	7.62	4.0
U	-	-	-	3.39	4.6	-	-
Eu	-	-	-	-	-	0.70	4.3
Hf	-	-	-	-	-	2.98	4.5
Tb	-	-	-	-	-	0.37	10.3
Yb	-	-	-	-	-	-	-
P	454	-	-	-	-	-	-
Ta	-	-	-	-	-	0.62	7.4

Table C 3 Measured and nominal composition of Skanska concrete.

				[w%]		
Element	**PGAA**	**Unc. %**	**XRF**	**Unc. %**	**NAA**	**Unc. %**
H	0.35	2.1	-	-	-	-
C	0.55	57.1	-	-	-	-
Na	0.55	2.7	0.509	46.1	0.56	3.8
Al	2.59	2.6	4.878	15.7	-	-
Si	34.12	1.3	29.862	4.3	-	-
S	0.31	3.2	0.258	2.5	-	-
K	1.28	2.6	1.483	0.6	-	-
Ca	8.36	3.0	9.213	1.1	-	-
Ti	0.16	3.1	0.187	2.7	-	-
Mn	0.05	3.2	0.045	2.2	-	-
Fe	1.61	3.2	1.637	2.4	2.10	3.7
O	50.46	2.4	-	-	-	-
				[ppmw]		
B	25.2	1.3	-	-	-	-
Cl	151.0	1.8	140	7.1	-	-
V	-	-	64.0	11.7	-	-
Sm	1.7	1.9	-	-	2.25	4.0
Gd	2.2	6.0	-	-	-	-
Mg	-	-	6357	15.7	-	-
Sc	-	-	-	-	4.75	3.6
Cr	-	-	63.6	3.5	109.80	3.9
Co	-	-	-	-	7.69	4.1
Ni	-	-	9.3	6.3	-	-
Cu	-	-	17.3	4.9	-	-
Zn	-	-	53.4	3.4	65.70	8.0
Ga	-	-	4.0	6.5	-	-
Ge	-	-	1.7	13.8	-	-
As	-	-	2.0	4.9	-	-
Rb	-	-	54.6	1.1	65.94	7.8
Sr	-	-	171.1	0.7	-	-
Y	-	-	15.1	2.7	-	-
Zr	-	-	145.4	0.3	-	-
Nb	-	-	4.9	2.3	-	-
Mo	-	-	3.0	5.6	-	-
In	-	-	1.1	9.4	-	-
Sn	-	-	1.5	18.0	-	-
Sb	-	-	1.3	15.3	1.33	11.3
Cs	-	-	1.9	11.3	1.10	10.9
Ba	-	-	386.7	0.4	404.70	5.9
La	-	-	16.1	2.7	14.62	3.9
Ce	-	-	28.5	2.1	38.90	4.2
Pr	-	-	4.9	11.3	-	-
Nd	-	-	16.7	5.6	17.29	9.1
W	-	-	-	-	174.70	3.8
Pb	-	-	12.6	4.7	-	-
Th	-	-	3.0	7.7	6.10	4.1
U	-	-	-	-	-	-
Eu	-	-	-	-	0.62	4.5
Hf	-	-	-	-	4.70	5.9
Tb	-	-	-	-	0.43	9.4
Yb	-	-	-	-	1.69	5.4
Ta	-	-	-	-	0.40	10.0

References

[1] S. Peggs, *ESS Technical Design Report*. 2013.

[2] D. D. DiJulio *et al.*, "A polyethylene-B4C based concrete for enhanced neutron shielding at neutron research facilities," *Nucl. Instruments Methods Phys. Res. Sect. A Accel. Spectrometers, Detect. Assoc. Equip.*, vol. 859, no. March, pp. 41–46, 2017.

[3] D. D. DiJulio, C. P. Cooper-Jensen, I. Llamas-Jansa, S. Kazi, and P. M. Bentley, "Measurements and Monte-Carlo simulations of the particle self-shielding effect of B4C grains in neutron shielding concrete," *Radiat. Phys. Chem.*, vol. 147, no. December 2017, pp. 40–44, 2018.

[4] E. S. A. Waly and M. A. Bourham, "Comparative study of different concrete composition as gamma-ray shielding materials," *Ann. Nucl. Energy*, vol. 85, pp. 306–310, 2015.

[5] A. Yadollahi, E. Nazemi, A. Zolfaghari, and A. M. Ajorloo, "Optimization of thermal neutron shield concrete mixture using artificial neural network," *Nucl. Eng. Des.*, vol. 305, pp. 146–155, 2016.

[6] V. P. Singh, A. M. Ali, N. M. Badiger, and A. M. El-Khayatt, "Monte Carlo simulation of gamma ray shielding parameters of concretes," *Nucl. Eng. Des.*, vol. 265, pp. 1071–1077, 2013.

[7] S. J. Park, J. G. Jang, and H. K. Lee, "Computational investigation of the neutron shielding and activation characteristics of borated concrete with polyethylene aggregate," *J. Nucl. Mater.*, vol. 452, no. 1–3, pp. 205–211, 2014.

[8] R. Tesse, F. Stichelbaut, N. Pauly, A. Dubus, and J. Derrien, "GEANT4 benchmark with MCNPX and PHITS for activation of concrete," *Nucl. Instruments Methods Phys. Res. Sect. B Beam Interact. with Mater. Atoms*, vol. 416, no. December 2017, pp. 68–72, 2018.

[9] E. Dian, K. Kanaki, R. J. Hall-Wilton, P. Zagyvai, and S. Czifrus, "Neutron activation and prompt gamma intensity in Ar/CO 2 -filled neutron detectors at the European Spallation Source," *Appl. Radiat. Isot.*, vol. 128, no. June, pp. 275–286, 2017.

[10] R. J. McConn Jr, C. J. Gesh, R. T. Pagh, R. A. Rucker, and R. G. Williams III, "Compendium of Material Composition Data for Radiation Transport Modeling," Richlnad, 2011.

[11] S. Alhajali, S. Yousef, and B. Naoum, "Appropriate concrete for nuclear reactor shielding," *Appl. Radiat. Isot.*, vol. 107, pp. 29–32, 2016.

[12] M. V. F. P. A. Lavdanskij, V. M. Nazarov, N. I. Stefanov, "Neutron activation analysis for determination of induced radioactivity in concrete of nuclear reactor shielding," *J. Radioanal. Nucl. Chem. Artic.*, vol. 131, no. 2, pp. 261–270, 1989.

[13] "Home | Budapest Neutron Centre." [Online]. Available: https://www.bnc.hu/. [Accessed: 02-Aug-2019].

[14] L. Szentmiklósi, T. Belgya, Z. Révay, and Z. Kis, "Upgrade of the prompt gamma activation analysis and the neutron-induced prompt gamma spectroscopy facilities at the Budapest research reactor," *J. Radioanal. Nucl. Chem.*, vol. 286, no. 2, pp. 501–505, 2010.

[15] L. Szentmiklósi, D. Párkányi, and I. Sziklai-László, "Upgrade of the Budapest neutron activation analysis laboratory," *J. Radioanal. Nucl. Chem.*, vol. 309, no. 1, pp. 91–99, 2016.

[16] A. Iida, "Synchrotron Radiation X-Ray Fluorescence Spectrometry," in *Encyclopedia of*

Analytical Chemistry, Chichester, UK: John Wiley & Sons, Ltd, 2000, pp. 1–23.

[17] B. Maróti, Z. Révay, L. Szentmiklósi, K. Kleszcz, D. Párkányi, and T. Belgya, "Benchmarking PGAA, in-beam NAA, reactor-NAA and handheld XRF spectrometry for the element analysis of archeological bronzes," *J. Radioanal. Nucl. Chem.*, vol. 317, no. 2, pp. 1151–1163, 2018.

[18] Z. Feng and L. Jun-Tao, "Monte Carlo simulation of PGNAA system for determining element content in the rock sample," *J. Radioanal. Nucl. Chem.*, vol. 299, no. 3, pp. 1219–1224, 2014.

[19] G. Mckinney, *MCNPX User's Manual, Version 2.7.0*. 2011.

[20] P. M. W. B. Wilson, S. T. Cowell, T. R. England, A. C. Hayes, *A Manual for CINDER'90 Version 07.4 Codes and Data LA-UR-07-8412*. Los Alamos National Laboratory, 2008.

[21] F. Corte, L. Moens, A. Simonits, A. Wispelaere, and J. Hoste, "Instantaneous α-determination without Cd-cover in the 1/E1+α epithermal neutron spectrum," *J. Radioanal. Chem.*, vol. 52, no. 2, pp. 295–304, Sep. 1979.

[22] F. De Corte *et al.*, "Installation and calibration of Kayzero-assisted NAA in three Central European countries via a Copernicus project.," *Appl. Radiat. Isot.*, vol. 55, no. 3, pp. 347–54, Sep. 2001.

[23] G. L. Molnar, *Handbook of prompt gamma activation analysis with neutron beams*. Kluwer Academic Publishers, 2004.

[24] "Seibersdorf laboratories | IAEA." [Online]. Available: https://www.iaea.org/about/organizational-structure/department-of-nuclear-sciences-and-applications/seibersdorf-laboratories. [Accessed: 02-Aug-2019].

[25] "Epsilon 5 integrated X-ray analysis system." [Online]. Available: http://www.speciation.net/Database/Instruments/PANalytical-BV/Epsilon-5-;i1663. [Accessed: 02-Aug-2019].

[26] U. Cevik, S. Akbulut, Y. Makarovska, and R. Van Grieken, "Polarized-beam high-energy EDXRF in geological samples," *Spectrosc. Lett.*, vol. 46, no. 1, pp. 36–46, 2013.

[27] R. J. McConn Jr, C. J. Gesh, R. T. Pagh, R. A. Rucker, and R. G. Williams III, "Compendium of Material Composition Data for Radiation Transport Modeling," Richlnad, 2011.

[28] E. Zanini, L.; DiJulio, D.; Santoro, V.; Bentley, P.; Klinkby, "Neutronic design of the bunker wall and roof," 2018.